

**ASSESSING THE DENDROCHRONOLOGICAL AND
DENDROCLIMATIC POTENTIAL OF SHASTA RED FIR (*Abies
magnifica* var. *shastensis*) IN NORTHERN CALIFORNIA AND
SOUTHWESTERN OREGON, USA**

A THESIS SUBMITTED TO THE FACULTY OF THE GRADUATE
SCHOOL OF THE UNIVERSITY OF MINNESOTA

BY MAX C.A. TORBENSON

IN PARTIAL FULFILLMENT OF THE REQUIREMENTS FOR THE
DEGREE OF
MASTER OF ARTS

JUNE 2014

DR. SCOTT ST. GEORGE

ACKNOWLEDGEMENTS

First and foremost I would like to thank my advisor, Dr. Scott St. George, whose help prior to, during, and after my time in Minnesota has been extraordinary. This thesis would not have been possible without his guidance. I am a better student and person because of it. I want to express my sincere gratitude for the wisdom bestowed upon me by Dr. Kurt Kipfmueller, ranging from discussions on research to introducing me to my favorite beverage. Thanks also go out to my final committee member, Dr. Emi Ito, for insightful input on my thesis and for providing a scientific safe haven (in the form of the QP community) for a student in minority.

Dr. Calvin Farris gave invaluable help during the planning stages of this research, as well as in the field. I thank Sarah Appleton and Jennifer Cribbs for backbreaking labor during the collection of samples. I am also in debt to Dr. Christopher Crawford, who throughout my degree has acted as a sounding board, as well as fellow lab members Lane, Megan and Erika. I gratefully acknowledge the financial support from the National Park Service, the UMn Department of Geography and the UMn Quaternary Paleoecology minor.

Sist men inte minst vill jag tacka mina föräldrar för allt stöd de givit mig under de senaste två åren.

ABSTRACT

We developed five ring-width records from Shasta red fir (*Abies magnifica* var. *shastensis*) stands in northern California and southwestern Oregon to evaluate growth trends and their relation to climate across the species' latitudinal range. The chronologies are made up of 173 trees in total, and earliest adequate replication ranges from AD 1624 to AD 1812. The oldest tree sampled has an inner-ring date of AD 1340. Tree age is only weakly correlated with size, and younger individuals (<300 years old) make up the majority of large trees (>100 cm DBH) in our data. Chronologies display shared variability in ring-width at inter-annual timescales; however, cross-dating across the full study region is not possible. The five records, together with one publicly available chronology, were compared to local and regional climate data. Significant correlations between red fir tree growth and local climate were found at all six sites but these relationships were not consistent throughout the latitudinal gradient. Prior analysis has suggested that the growth of the species is primarily limited by summer minimum temperature, but this relationship was not apparent at most sites within our network. Instead, the associations observed between red fir growth and climate are multivariate, dependent on the temporal resolution of climate data used, and may also be influenced by both latitude and elevation.

TABLE OF CONTENTS

List of tables.....	iv
List of figures.....	v
Introduction.....	1
Study region.....	3
<i>Climate</i>	3
Data.....	8
<i>Site descriptions</i>	8
<i>Climate data</i>	10
Methods.....	12
<i>Laboratory methods</i>	12
<i>Analytical methods</i>	12
Results.....	14
<i>Shasta red fir growth-climate relationship</i>	28
Discussion.....	37
<i>Interpreting the climate signal in Shasta red fir</i>	40
Conclusion.....	43
<i>Future research</i>	44
References.....	46

LIST OF TABLES

Table 1 – Geographical and tree-ring data.....	9
Table 2 – Characteristics of climate data.....	9
Table 3 – Characteristics of tree-ring chronology data.....	16
Table 4 – Correlation matrix for Shasta red fir chronologies.....	16

LIST OF FIGURES

Figure 1 – Climograph for Oregon climate division 3.....	6
Figure 2 – Time series of Mount Shasta winter precipitation.....	7
Figure 3 – Map of site locations sampled.....	8
Figure 4 – Images of settings of trees sampled.....	11
Figure 5 – Ring count-DBH scatterplot.....	17
Figure 6 – Plot of six Shasta red fir chronologies.....	18
Figure 7 – Plot of different chronologies from Grey Back Meadow.....	19
Figure 8 – Images of most recent growth.....	22
Figure 9 – Images of traumatic resin ducts.....	23
Figure 10 – Temporal distribution of traumatic resin ducts at Shasta red fir sites.....	24
Figure 11 – Trend in traumatic resin ducts at Reading Peak and Diamond Peak.....	25
Figure 12 – Age-distribution of traumatic resin ducts.....	26
Figure 13 – Traumatic resin ducts by age class.....	27
Figure 14A – Climate-growth correlations at Cinnamon Butte.....	30
Figure 14B – Climate-growth correlations at Grey Back Meadow.....	32
Figure 14C – Climate-growth correlations at Mount Ashland.....	33
Figure 14D – Climate-growth correlations at Shasta Grey Butte.....	34
Figure 14E – Climate-growth correlations at Reading Peak.....	35
Figure 14F – Climate-growth correlations at Diamond Peak.....	36
Figure 15 – Observed ring counts in Shasta red fir versus predicted age.....	39

INTRODUCTION

A long-term perspective, going back further in time than the observational record allows, is crucial to understand climate variability in any given region. Most climate records span less than a century (e.g. Menne *et al.* 2009), so observations are not able to describe the full variability of the climate system, particularly in the absence of major anthropogenic interference. Proxy records are therefore used to extend our observational recordings of climate (Bradley 2008). Climate proxies come in many forms including speleothems, lake cores, corals and tree-rings and each type of proxy has advantages and disadvantages associated (Bradley 1985). Trees provide a unique spatiotemporal perspective because of the annual nature of their growth layers and wide spatial distribution throughout most of the terrestrial landscape (Fritts 1976). Several thousand tree-ring chronologies have been developed across the world (Grissino-Mayer and Fritts 1997) but there are geographical differences in the response of tree growth to climate (St. George and Ault 2014), as well as species-specific differences (e.g. Villalba *et al.* 1994). Numerous species on the West Coast of the United States have previously been used in dendroclimatic research (Briffa *et al.* 1992) and although some studies have yielded considerable success (Stahle *et al.* 2011), chronologies developed in higher elevation areas tend to contain less distinct climate signals (Graumlich 1993; Peterson and Peterson 2001; Peterson *et al.* 2002; Gedalof *et al.* 2004).

Winter precipitation on the central Pacific Coast (CPC) has shown a rare decadal pattern during the last 100 years (St. George and Ault 2011). The pattern has had a large influence on water scarcity in California and Oregon, and is therefore of

great interest to not only paleoclimatologists but also water resource managers and in the region. Previously constructed tree-ring chronologies have been used as proxies in attempts to extend the instrumental record with the purpose of studying the stability of these decadal swings in climate. However, records that show high correlation with the decadal signal are limited to a single species that grow in low-elevation valley landscapes (St. George and Ault 2011; Stahle *et al.* 2011). Developing new tree-ring records that have the potential of containing information on the decadal pattern in other locales is crucial for understanding the temporal stability of climate in the region.

Red fir (*Abies magnifica*) and the subspecies Shasta red fir (*A. magnifica* var. *shastensis*) is endemic to the U.S. West Coast and can be found in forests and meadow edges in the Sierra Nevada, the Cascades and the Klamath Mountains (Barbour and Woodward 1985; Sawyer and Thornburgh 1988). Forests at elevations between 1500 and 2700 m receive the most snowpack of any forest type in California and because of its tolerance of snow, red fir occurs in pure stands throughout much of that elevational zone (Oostings and Billings 1943). Snowpack depth can reach over 5 m in depth in red fir stands and it has been proposed that the timing of snowmelt is a key parameter for the growth of the species (Royce and Barbour 2001). Zhang and Oliver (2006) suggested the importance of growing season minimum temperature on red fir growth variability but their comparison was limited to a 31-year overlap, which may fail to capture the impact of low-frequency climate patterns. Furthermore, the study was limited to 10 trees from a single site (Swain Mountain Experimental

Forest, California) and therefore, these results may not be representative for the full distribution of the species.

In this paper we present five new Shasta red fir chronologies spanning the species latitudinal range. The potential dendroclimatic information stored in these trees could be of great value in understanding the regional climate stability due to the species' success in environments where winter precipitation demonstrates the most pronounced decadal behavior. The synchronicity of radial growth variability is assessed and we show that the trees show significant coherency in growth across space. The relationship between inter-annual growth and local and regional climate is analyzed. This more extensive comparison does not support previous suggestions that a single climate variable alone has exerted enough stress on growth during the last 115 years for the climate variable to be picked up in the tree-ring record consistently. In addition, we also analyze growth anomalies present in our samples and examine the age-size relationship in red fir trees.

STUDY REGION

The CPC is made up of a complex pattern of geological features, with several mountain ranges dominating the region. The Cascades are the most prominent of these ranges and spans a distance of over 1,000 km from Mount Garibaldi in British Columbia to Lassen Peak in California. Tectonic activity continues to play an important role in landscape evolution, both on and offshore, and several volcanoes have been active within the last thousand years, including Mount Shasta and Lassen Peak (Westhusing 1973).

Climate

The climate of the CPC is characterized by cool, wet winters and warm, dry summers (Rocherford *et al.* 1994, **Figure 1**). Precipitation is highly seasonal and the majority of moisture is received during the winter months. Up to 90% of the annual precipitation in high-elevation areas (>2000 m) falls as snow (Gordon 1979). The El Niño Southern Oscillation (ENSO) has a large influence on winter precipitation over western United States (Cayan *et al.* 1999), and the June-November Southern Oscillation Index (SOI) explains up to 25% of the variance in October-March precipitation (Wise 2010). The Pacific Decadal Oscillation and Atlantic Multidecadal Oscillation has also been suggested as important drivers of hydroclimatic variability (McCabe *et al.* 2007; Higgins *et al.* 2007) in the region. However, the relationship between these multiannual oscillations and precipitation across the U.S. West Coast is not stable across space. Instead, the association takes form of a dipole where precipitation in the Pacific Northwest shows positive correlation with the SOI and the Desert Southwest negative correlation. The CPC lies in the transition zone of this dipole and does not show a consistent response to ENSO (Wise 2010).

The 20th and early 21st century observed winter precipitation for the CPC has shown some of the largest decade-to-decade variability in North American climate (Ault and St. George 2010, **Figure 2**). These decadal swings have had a major impact on water resources and have been identified in discharge records of the Sacramento-San Joaquin River system (Florsheim and Dettinger 2007; St. George and Ault 2011). Observations show that this pattern began in the 1930s, and tree-ring reconstructions indicate that the behavior did not occur prior to the 20th century; however, few

suitable high-resolution proxy records exist from northern California, the epicenter of the signal (St. George and Ault 2011). The Southern Cascades acts as a topographic boundary to moisture moving onshore and creates one of the biggest rain-shadow effect of any of the coastal mountain ranges on the U.S. West Coast (Skinner and Taylor 2006). Valleys and lowlands experience less rain and snow than the high elevation areas. An example of the spatial variability in winter precipitation is evident when comparing mean April 1st snow water equivalent (SWE) at Burney Springs (50 mm), east of the mountains, and Stouts Meadow (950 mm), only 25 km to the west (California Data Exchange Center; CDEC). The spatial variability of precipitation dictates the broader patterns of vegetation cover in the region. The spatial variability of precipitation dictates the broader patterns of vegetation cover in the region. To the east of the mountain range, steppe-like conditions dominate and many of the species found west of the mountains cannot tolerate the drier conditions here (Riegel *et al.* 2006). To the west, a variety of tree species can be found at higher elevations, including ponderosa pine (*Pinus ponderosa*), Douglas-fir (*Pseudotsuga menziesii*), mountain hemlock (*Tsuga mertensiana*), white fir (*Abies concolor*), Jeffrey pine (*Pinus jeffreyi*), and red fir.

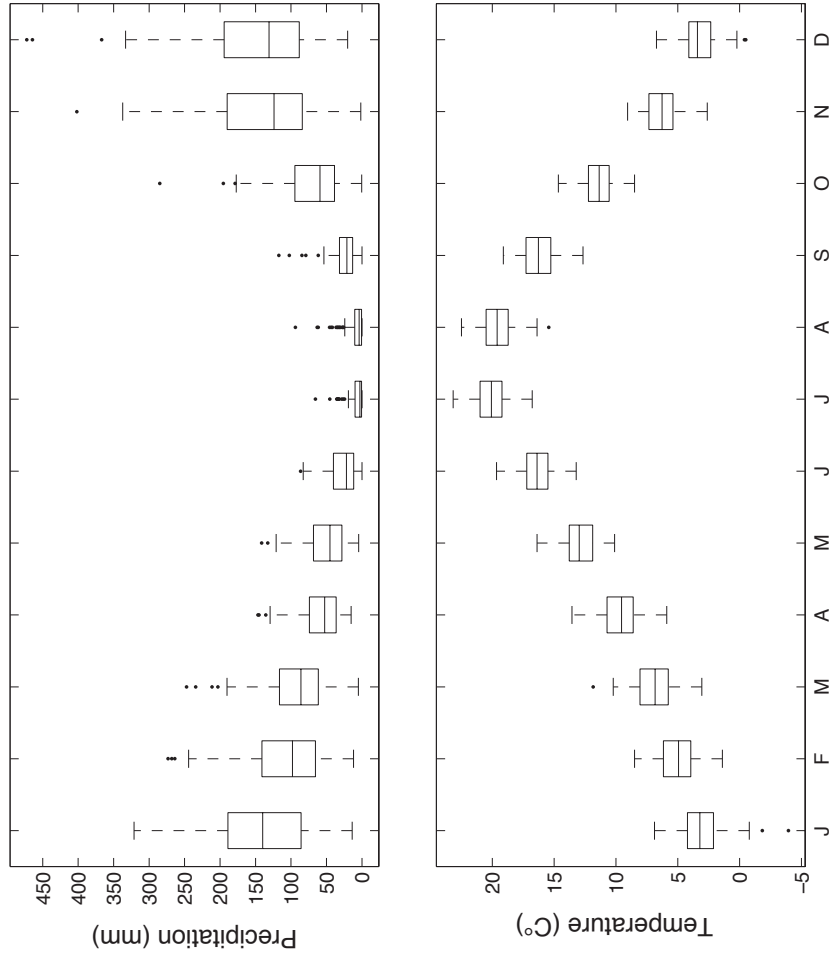


Figure 1. Climograph (for period 1895-2012) displaying the monthly mean and range of precipitation (above) and mean temperature (below) of Oregon climate division of 3. Black dots denote outliers.

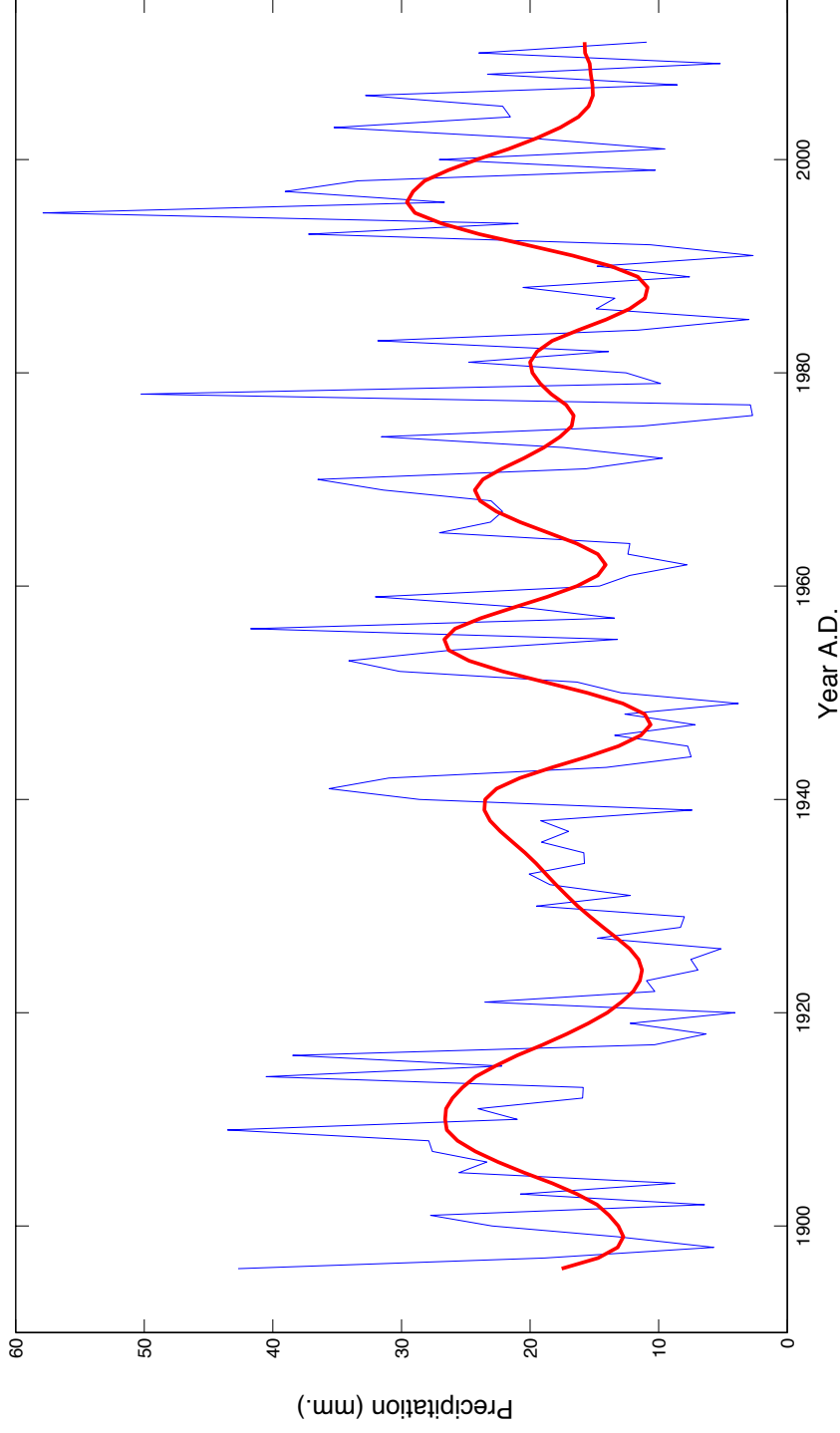


Figure 2. Time series of Mount Shasta HCN station winter (DJF) precipitation from the United States Historical Climate Network (Menne *et al.* 2009). The red line denotes the decadal variability of the time series, extracted through Singular Spectrum Analysis.

DATA

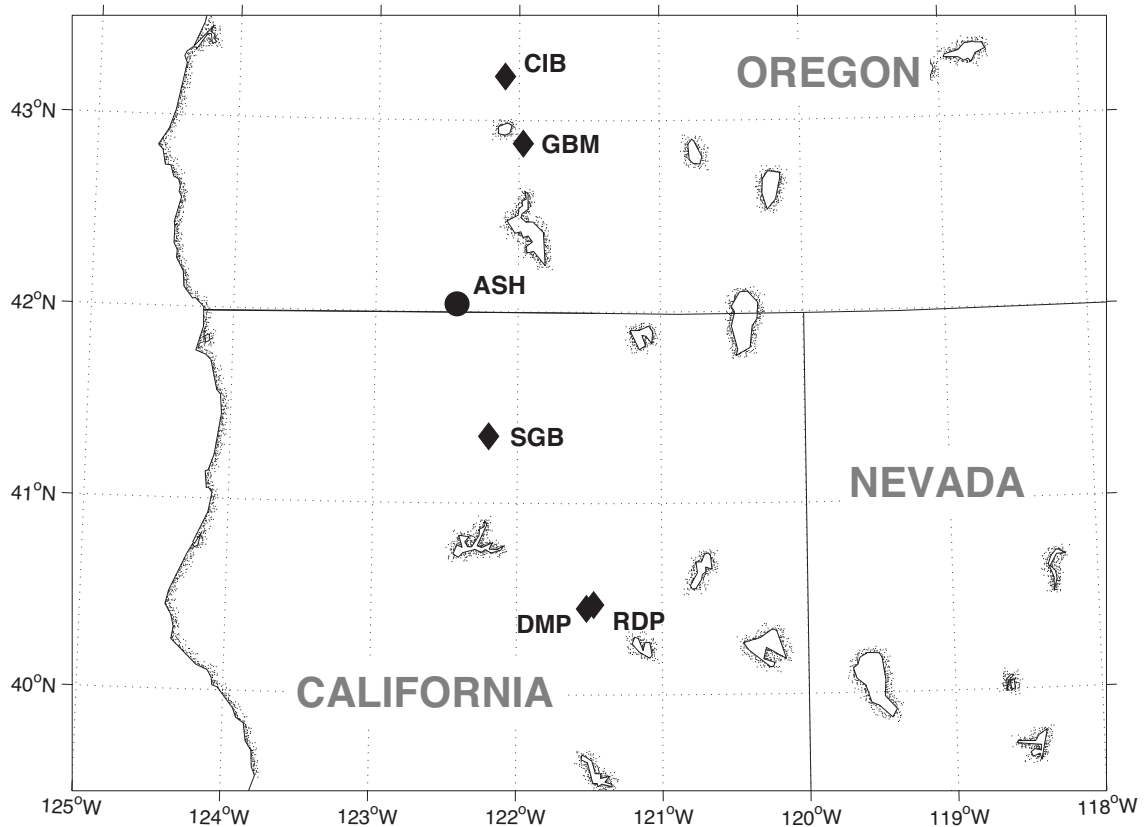


Figure 3. Tree-ring site locations sampled for Shasta red fir in this study. Diamonds indicate the locations of new records, and the circle indicates the location of the record produced by Schweingruber (1988).

Site descriptions

Identification of sampling sites was made possible through examination of satellite imagery and collaboration with personnel from the National Park Service. We selected sites based on geographical location, the presence of old-growth trees, canopy setting, and absence of recent disturbances. Five sites hosting Shasta red fir stands that met our criteria were identified along a north-south gradient, spanning latitudes 40.45 and 43.25 °N (**Figure 3; Table 1**). The elevation of sites ranges from 1,800-2,400 m. Trees grew at

Site code	Site name	Protected area	Lat. (°N)	Lon. (°W)	Elev. (m)	Trees	Radii	Source
CIB	Cinnamon Butte	Umpqua N.F.	43.23	122.10	1800	37	64	This study
GBM	Grey Back Meadows	Crater Lake N.P.	42.88	122.07	2050	30	58	This study
ASH	Mount Ashland	Klamath N.F.	42.04	122.43	1860	11	22	Schweingruber (1988)
SGB	Shasta Grey Butte	Shasta-Trinity N.F.	41.35	122.20	2425	30	54	This study
RDP	Reading Peak	Lassen Volcanic N.P.	40.47	121.47	2285	36	69	This study
DMP	Diamond Peak	Lassen Volcanic N.P.	40.45	121.52	2300	40	72	This study

Table 1. Meta-data describing the geographical location and characteristics of Shasta red fir tree-ring samples used in this study.

Variable	Spatial resolution	Temporal resolution	Start year	End year	Source
Temperature and precipitation	Station	Monthly	1895	2011	USHCN
Temperature and precipitation	4x4 km	Monthly	1895	2011	PRISM
Snow Water Equivalent	Station	Point	1930	2010	CDEC
Temperature and precipitation	Division	Monthly	1895	2011	NCDC
PDSI and PHDI	Division	Monthly	1895	2011	NCDC

Table 2. Characteristics of climate data used in this study.

the fringes of meadows as well as on slopes and rock outcrops (**Figure 4**). At each site, increment cores from 30 to 40 living trees were taken at breast height along two radii of the tree. Our sampling strategy targeted trees that had the physical characteristics to suggest they were of the greatest age (Pederson 2010) and favored open-grown individuals without visible injuries. Diameter at breast height (DBH), relative position, and crown characteristics were among supplementary data collected for each tree. Ring-width data from an additional site near Mount Ashland, Oregon (site code: OR044) were obtained from the International Tree-Ring Data Bank (Grissino-Mayer and Fritts 1997), developed by Schweingruber (1988).

Climate data

Local observational data were obtained from the United States Historical Climatology Network (USHCN; Menne *et al.* 2009) and CDEC. Gridded data came from the Parameter-elevation Regressions on Independent Slopes Model (PRISM; Daly *et al.* 2008). Gridded climate series were taken from either the closest grid point to the site or were combined from the closest grid points forming a square centered on the site. Data for California climate division 2 and Oregon climate division 3 were acquired from the National Climatic Data Center (NCDC). Climate variables analyzed include temperature, precipitation, SWE, Palmer Drought Severity Index (PDSI) and Palmer Hydrological Drought Index (PHDI) (**Table 2**).

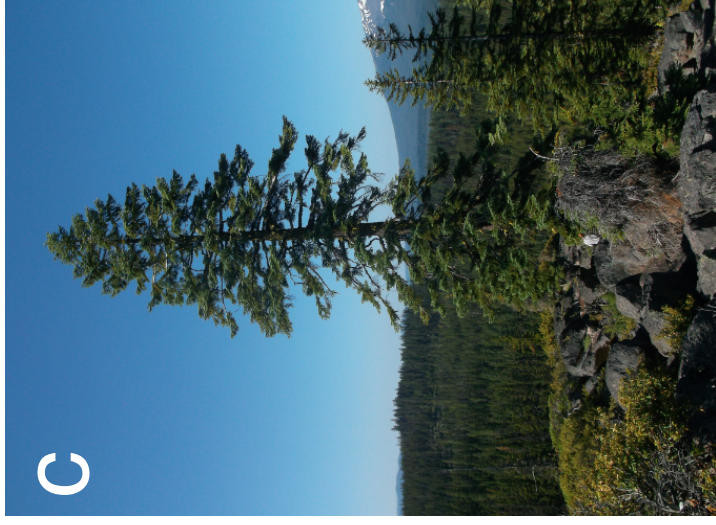


Figure 4. The settings of Shasta red fir trees sampled on the central Pacific Coast in this study included (a) meadow fringes, (b) slopes, and (c) rock outcrops.

METHODS

Laboratory methods

Cores were secured on wooden mounts and the surfaces of cores were prepared according to conventional dendrochronological methods (Stokes and Smiley 1968). Scalpel and sandpaper were used to produce greater clarity and detail in ring boundaries. Rings were counted, and each ring was assigned a calendric date using narrow rings as marker years (Yamaguchi 1986). Total ring widths (TRW) for each core were measured on a Velmex sliding measuring system. Initial crossdating of TRW series were statistically verified using COFECHA (Holmes 1986).

Analytical methods

Each measurement series was processed to estimate and remove the age-related trend inherent in most open-grown trees. As a tree grows, the amount of wood needed to cover the larger circumference increases, and thus radial growth decreases with age assuming wood production is constant (Fritts 1976). Series were converted to dimensionless indices by fitting growth curves to the data in ARSTAN (Cook and Holmes 1986). Several different detrending approaches including linear and negative exponential curves, and cubic splines of varying flexibility were used for series from each site in order to assess the impact of standardization choices on the variability and periodicity of the site-level composites. Indices from individual cores were averaged to create local chronologies, representing a site-scale departure from mean growth in any given year. The distribution of values for the instrumental period of each chronology was tested for normality using the Lilliefors test (Conover 1980).

The relationship between climate and TRW variability was primarily assessed through the computer code SEASCORR (Meko *et al.* 2011). SEASCORR is a MATLAB program that identifies the seasonal climate signal in annual tree-ring series and has been applied previously to tree-ring records from the Appalachian Mountains (Crawford 2012), Spain (Touchan *et al.* 2013) and northern Africa (Meko *et al.* 2011). The code uses correlation as a measure of similarity between variability in ring-width and climate, but also determines the relationship between the primary and secondary climate variables of interest (as defined by the user). The set of Shasta red fir chronologies were compared to temperature and hydroclimatic variables of ranging seasonal groupings. The temporal stability of the climate-TRW relationship was also addressed by testing the significance of differences between correlations calculated over two sub-periods (the calibration period divided in half). In addition to the individual site chronologies, the six chronologies were averaged to produce a regional chronology that was tested against the divisional climate data.

Rings containing traumatic resin ducts (TRDs) were recorded for each core and composite time series were constructed of the percentage of trees recording TRDs (due to varying sample depth throughout the period of study). The TRD time series were qualitatively compared to monthly precipitation and temperature data, and to daily climate data where available. The relative year of TRDs were also analyzed in order to assess the role of age in the occurrence of the growth anomaly.

RESULTS

Tree-ring characteristics

The average length of the TRW series from the six sites is 235 years and range between 181 (at Mount Ashland) to 320 years (Reading Peak). The longest individual series comes from Cinnamon Butte and is 672 years long, spanning AD 1340-2011. Ring counts (estimated age) were weakly correlated with DBH (**Figure 5**). Mean interseries correlation (\bar{r}) (Wigley *et al.* 1984) between trees at a single site range between 0.245 and 0.337, with the highest values produced by the Diamond Peak record. Six site chronologies were constructed (**Figure 6**), each representing the average growth of Shasta red fir at the site going back several centuries. Notable features in the records include a prolonged period of below-mean growth in the second and third decades of the 20th century present at the four southern sites. Trees at the four of the five sites that cover the early 21st century also show a decline in growth during the last decade. The records from Cinnamon Butte, Grey Back Meadow and Shasta Grey Butte also show a dip in growth after A.D. 1700; however, trees at Reading Peak and Diamond Peak are growing above average during this period. The Grey Back Meadow chronology displays negative departures from the mean in the mid-1800s; however, no other chronology displays this pattern and it can be assumed the event is of local nature. Although four of the six chronologies have a start date in the 1500s or earlier, no chronology is well replicated (Expressed Population Signal > 0.85 ; Wigley *et al.* 1984) prior to 1624 (**Table 3**). Choices in standardization of raw TRW measurements dictate the shape of the final site chronologies. Negative exponential and linear curves retain more of the low-

frequency pattern, while flexible splines accentuates the inter-annual variability. The differences are most noticeable where sample depth is low, including the early parts of the chronologies. Furthermore, less coherency towards the end of the series is observed between chronologies produced through different detrending options for sites with the lowest inter-series correlation (Cinnamon Butte and Grey Back Meadow; **Figure 7**). Standardization choices also affect the amount of autocorrelation in the chronologies. For example, the Shasta Grey Butte chronologies constructed using negative exponential curves and the stiffest cubic spline (200% of the individual series' length) have significant ($\alpha = 0.05$) autocorrelation in year 1, 3, 4, 6, and 7. When a more flexible spline is used (100% of the individual series' length) there is only significant autocorrelation in year 1. Similar but less drastic changes can be seen in the chronologies from Grey Back Meadow and Cinnamon Butte. However, several chronologies constructed using more flexible splines failed to meet the Lilliefors test for normality, and thus violate the assumption of normal distribution that underpins some of the further analysis (Meko *et al.* 2011).

Correlations between site chronologies range from 0.220 to 0.592 (**Table 4**). Diamond Peak and Reading Peak show the highest correlation (0.592) of any two chronologies but are also the sites with the shortest distance between them. The most southern site (Diamond Peak) shows correlations above 0.350 against all other chronologies. Shasta Grey Butte displays correlations above 0.420 against all chronologies except Grey Back Meadow.

Site code	Site chronology	Start year	End year	MSSL	rbar	EPS	Year EPS > 0.85
CIB	Cinnamon Butte	1340	2011	232	0.25	0.73	1800
GBM	Grey Back Meadows	1614	2011	193	0.29	0.82	1812
ASH	Mount Ashland	1739	1982	181	0.41	0.87	1831
SGB	Shasta Grey Butte	1551	2011	277	0.26	0.84	1767
RDP	Reading Peak	1513	2011	320	0.31	0.89	1624
DMP	Diamond Peak	1605	2011	209	0.34	0.89	1738

Table 3. Characteristics of tree-ring chronologies used in this study. Year EPS > 0.85 denotes the earliest year after which EPS continuously exceeds 0.85.

	CIB	GBM	SGB	RDP	DMP	ASH
CIB	X	0.52	0.43	0.30	0.41	0.42
GBM	0.52	X	0.22	0.29	0.36	0.35
SGB	0.43	0.22	X	0.46	0.50	0.48
RDP	0.30	0.29	0.46	X	0.59	0.38
DMP	0.41	0.36	0.50	0.59	X	0.47
ASH	0.42	0.35	0.48	0.38	0.47	X

Table 4. Correlation matrices for six Shasta red fir TRW chronologies from the central Pacific Coast. Correlations were computed for the longest possible overlap between chronologies.

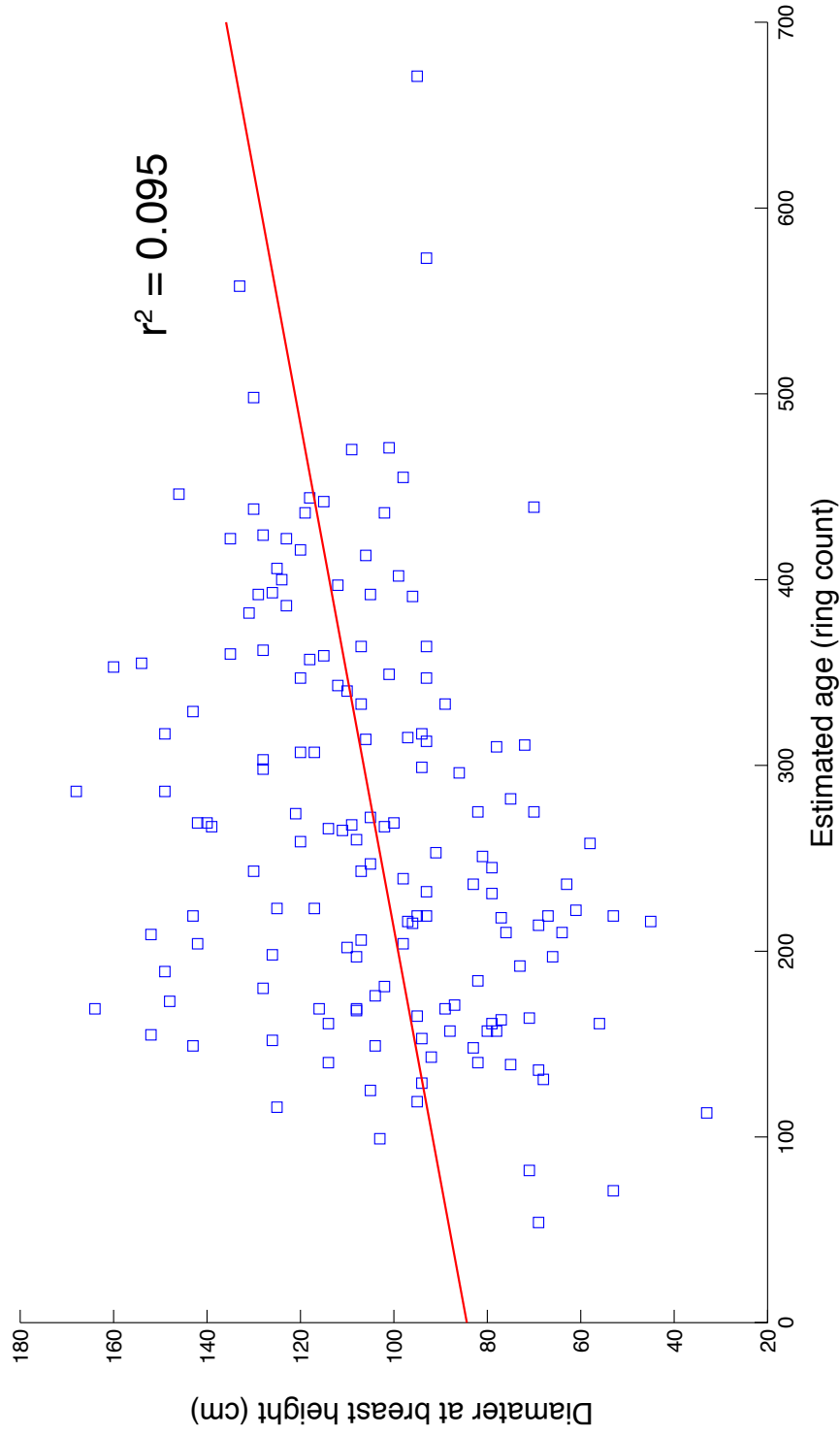


Figure 5. Scatterplot of estimated age (ring count) and size (DBH) of trees from the five Red fir collections presented in this study.

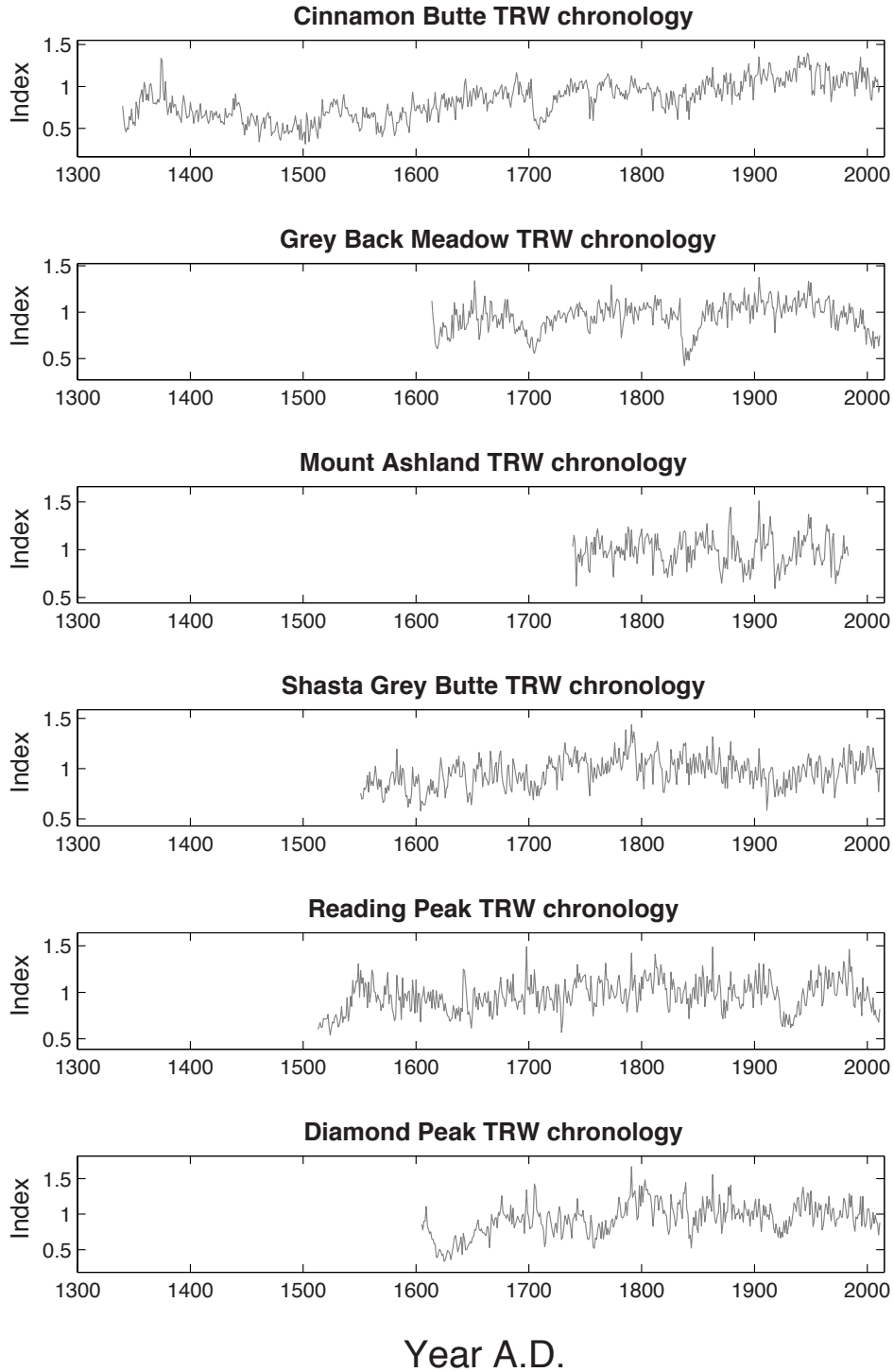


Figure 6. Time series describing mean (stand-average) TRW for Shasta red fir trees growing at six locations in southeastern California and southwestern Oregon.

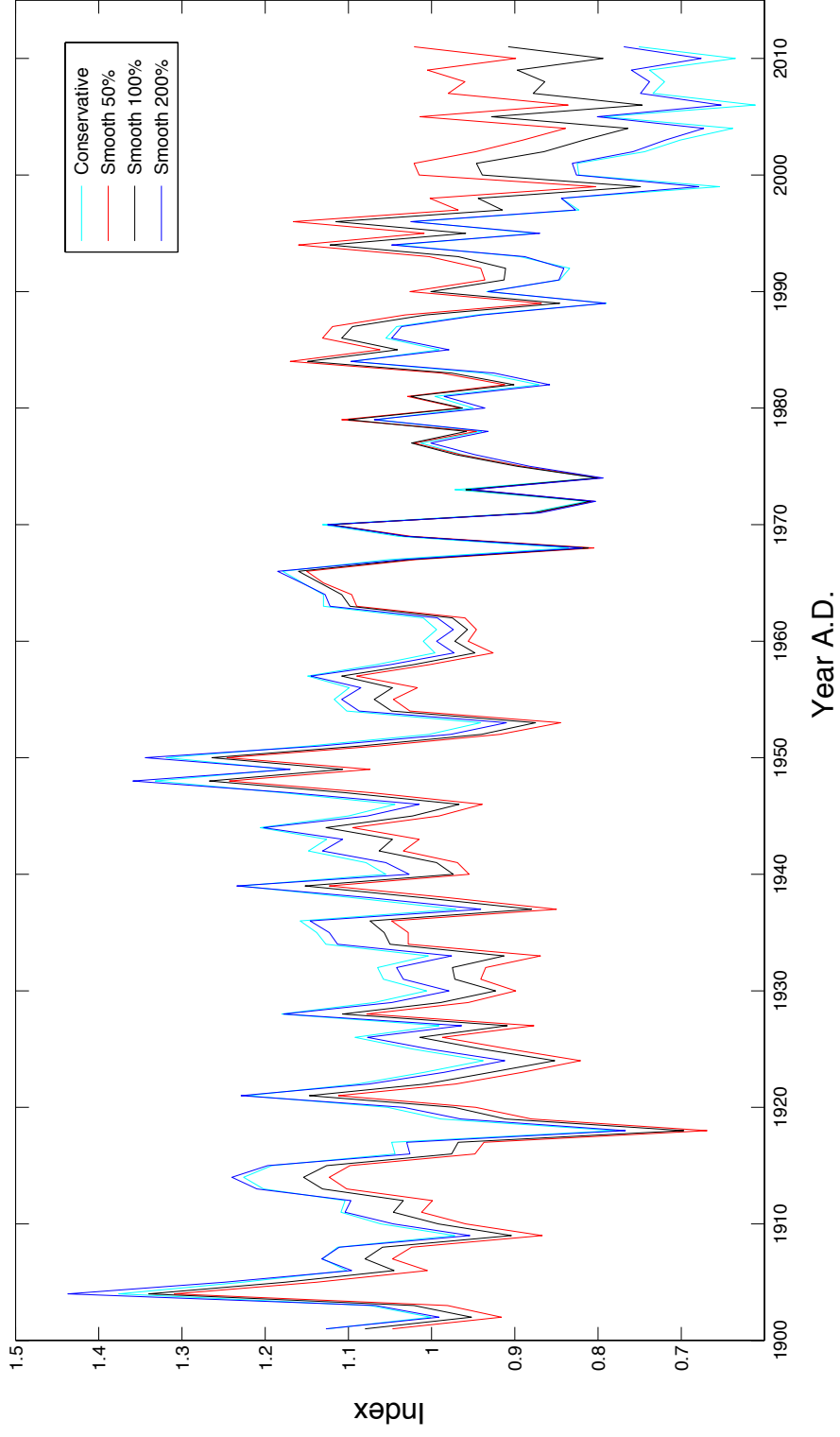


Figure 7. Ring-width series for Grey Back Meadow produced using a variety of detrending methods. The negative exponential curve and the 200% cubic spline accentuate the recent (last 15 years) trend of lower growth.

Many of the trees sampled had not started to produce a growth ring for 2012. The majority of exceptions to this pattern were trees found at Shasta Grey Butte, which was the last site to be sampled (in early August), and Reading Peak (**Figure 8A**). Why Reading Peak has many trees with initial growth and not nearby Diamond Peak (**Figure 8B**; **Figure 8C**) is yet to be determined. Grey Back Meadow was sampled at the end of July and several trees had yet to put on any earlywood cells (**Figure 8D**).

Trees from all five sites sampled by the authors contained traumatic resin ducts (TRD). TRDs are a type of growth anomaly characterized by an increase in resin ducts and the flushing of those ducts with resin, which is preserved in the wood. These features occur when a tree experiences one or more of a range of stresses (Schweingruber 2007), including mechanical injuries, beetle or fungi attacks, browsing by herbivores, and drought (Stoffel 2008). Of over 46000 rings analyzed in total, 1500 showed evidence of TRDs. The vast majority (>95%) of the TRDs occur in the earliest wood formed in the growing season (**Figure 9**). Fewer than 20% of TRDs are present in both cores from the same trees, and many tangential rows of TRDs do not cover the whole core surface. The high within-sample variation makes it difficult to draw conclusions about trends across the entire population and to extract any potential signal that could exist in the record. At the three northern-most sites (Cinnamon Butte, Grey Back Meadow and Shasta Grey Butte) the TRDs are evenly distributed over time (**Figure 10**). At Diamond Peak and Reading Peak, a positive trend ($p < 0.001$) in the number of trees recording TRDs is present during the 20th and early 21st century (**Figure 11**). Diamond Peak and Reading Peak are also the two sites

with the highest frequency of TRDs. Older trees were more likely to record the growth anomaly (**Figure 12**), and although sample depth was low ($n = 23$), the data indicate that it is the older trees that drive the recent positive trend (**Figure 13**). Some samples from Shasta Grey Butte showed evidence of TRDs in the developing 2012 growth layer, despite any visible damage to the trees. Thus, because the stresses described in previous research did not appear to have caused the anomalies, however no clear relationship was found between the presence of TRDs and temperature or precipitation. Furthermore, no relationship between the probability of a ring containing TRDs and its width was found. Therefore, the external variables controlling growth variability in Shasta red fir does not seem to control the formation of TRDs.

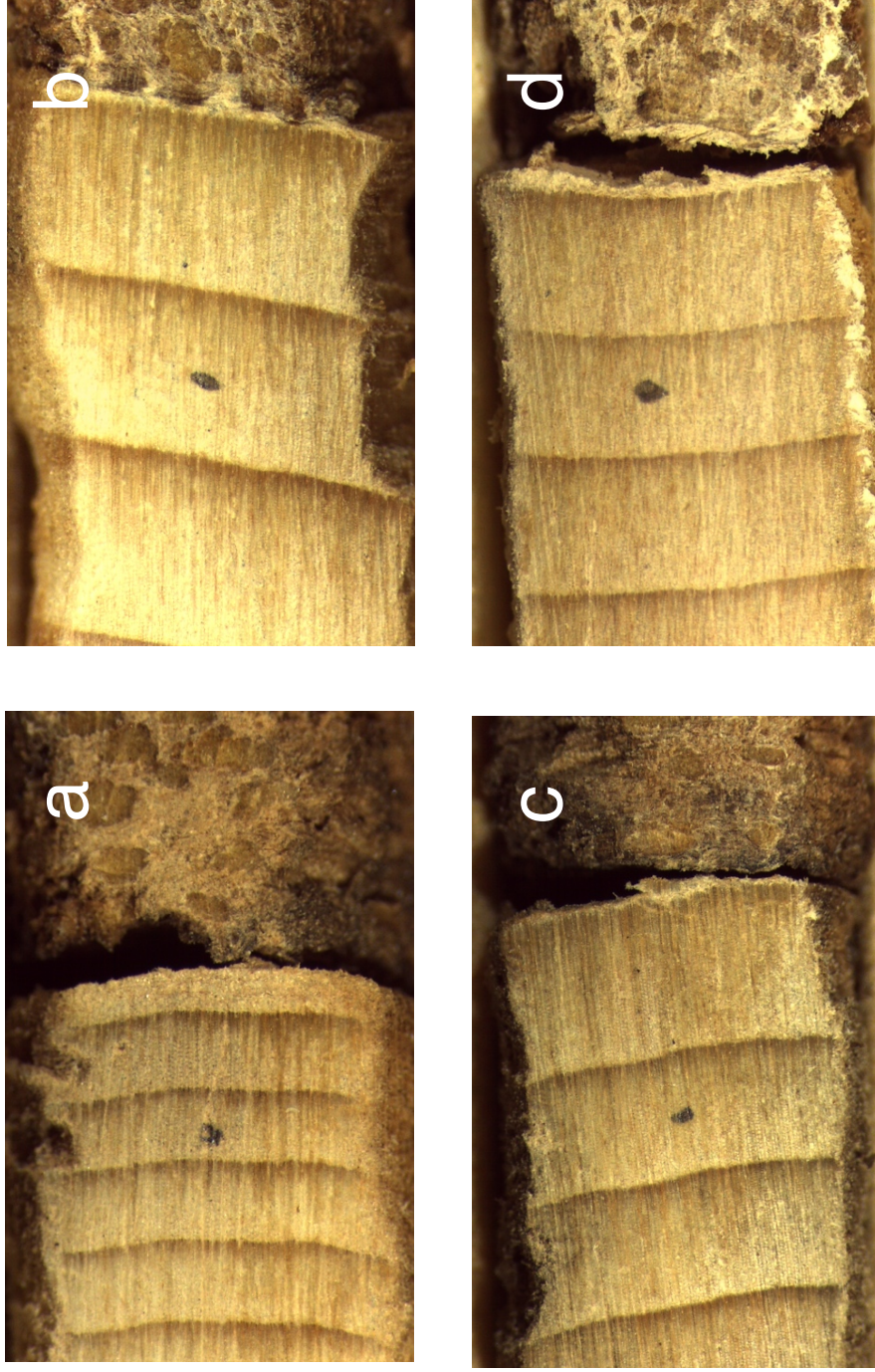


Figure 8. Photography of the most recent growth rings in Shasta red fir samples. Black dots mark the growth ring of year 2010. (a) Sample RDP025A, collected July 17th, shows several earlywood cells formed for 2012. (b) Sample DMP037A, collected July 14th, (c) sample DMP012A, collected July 13th, and (d) sample GBM001A, collected July 21st, show no signs of earlywood cells for 2012.

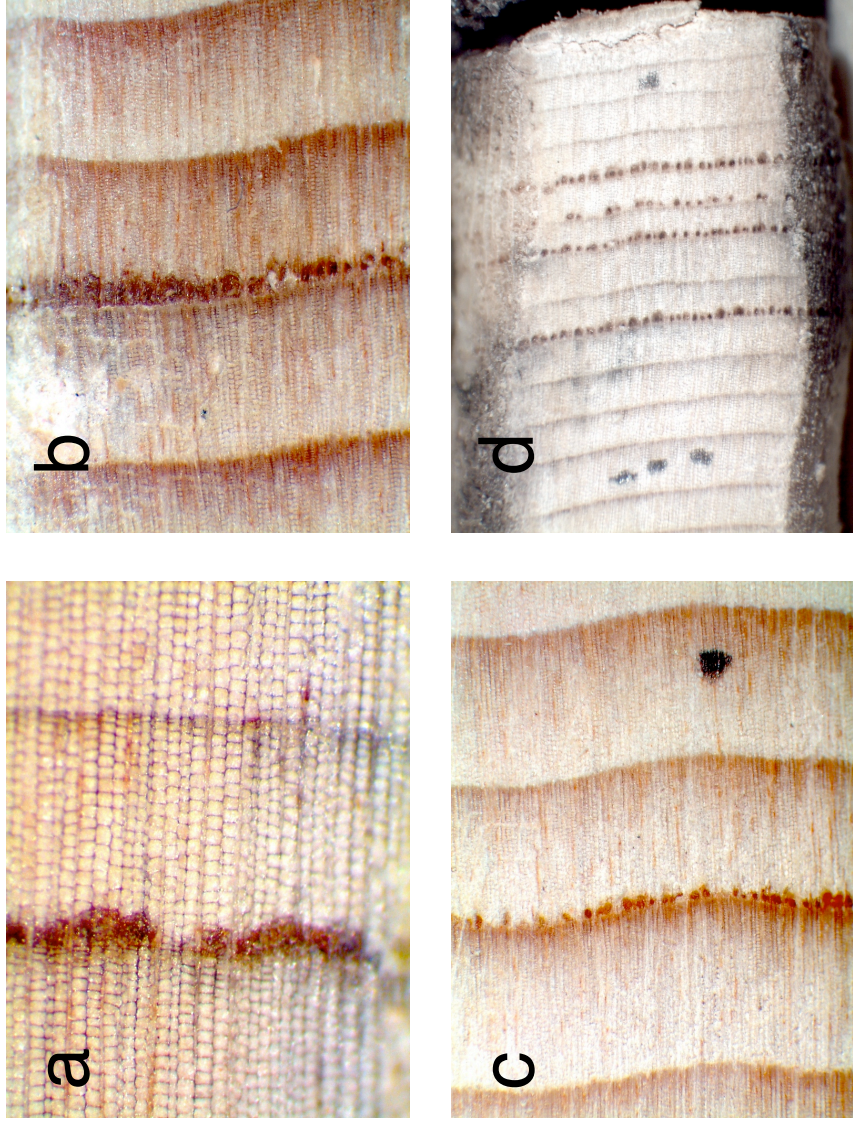


Figure 9. Photography of traumatic resin ducts in Shasta red fir samples, with growth from left to right. (a) Sample GBM023A showing TRDs in A.D. 1964. (b) Sample SGB018B showing TRDs in A.D. 1794. (c) Sample GBM018B showing TRDs in A.D. 1959. (d) Sample RDP017A showing TRDs in A.D. 2004, 2006, 2007 and 2008.

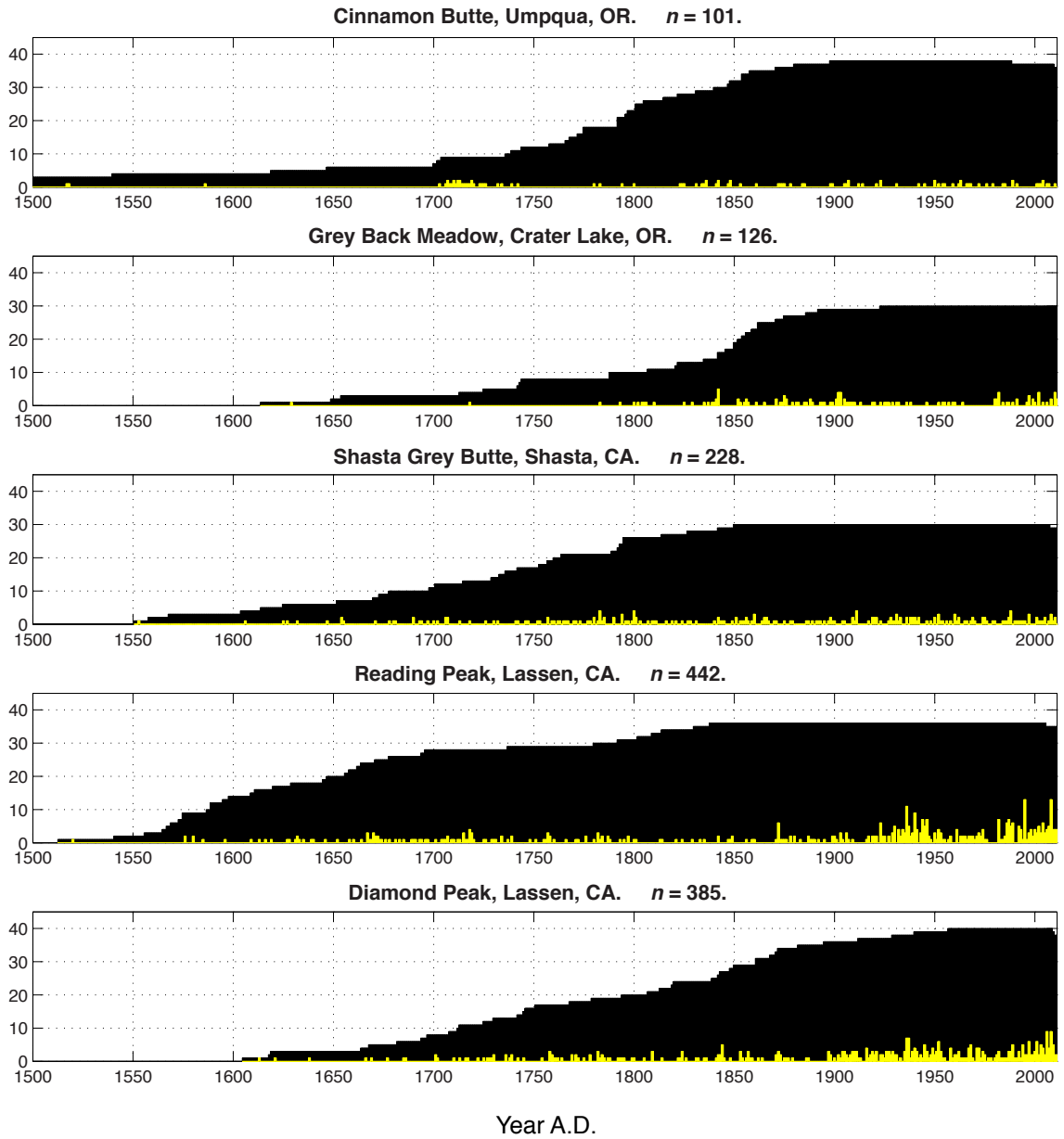


Figure 10. Frequency of TRDs at five Shasta red fir sites on the central Pacific Coast. The black bars indicate sample depth (trees) at given year and yellow indicates number of trees showing evidence of TRDs.

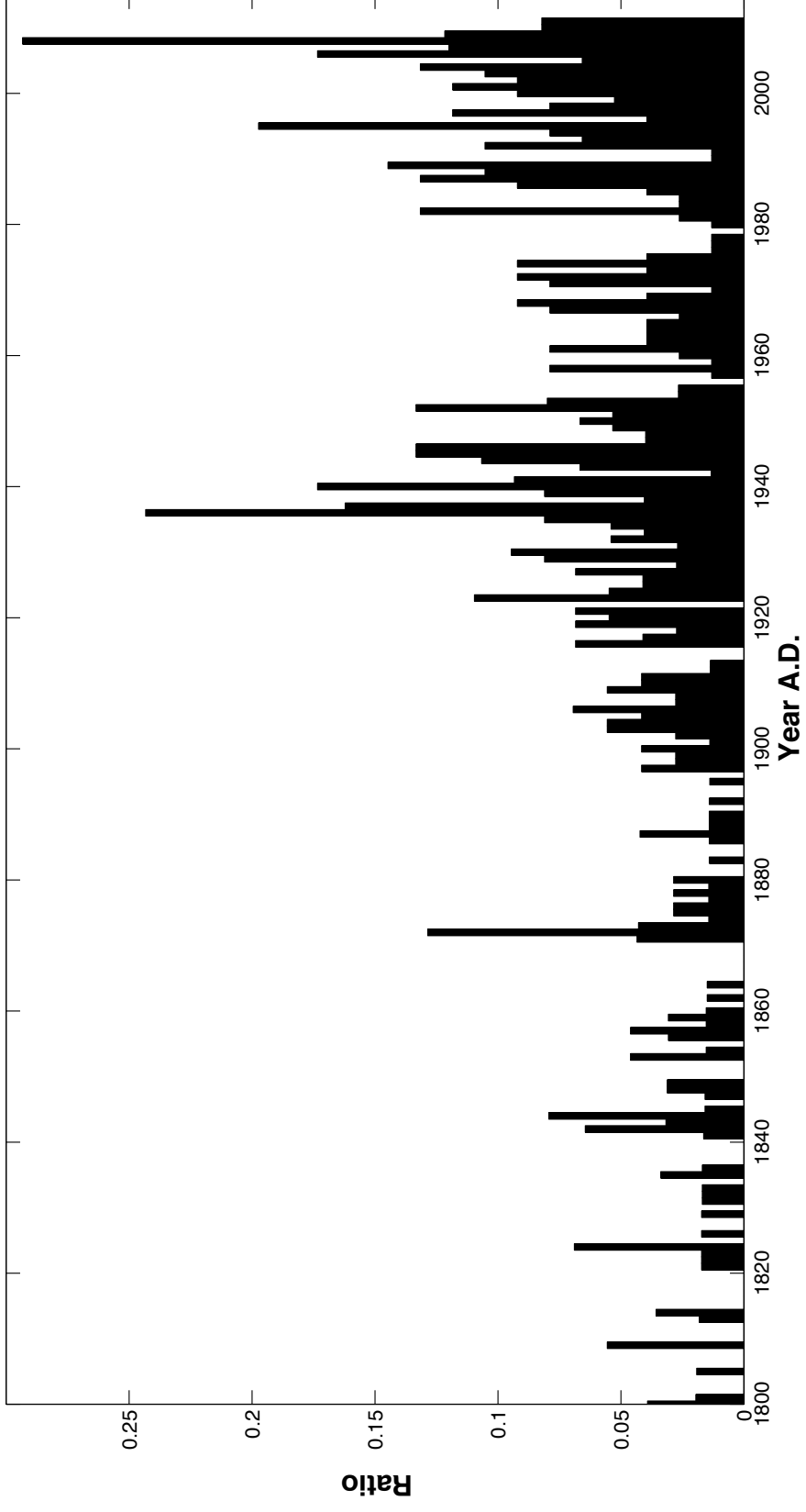


Figure 11. Ratio of trees from Diamond Peak and Reading Peak (combined) showing evidence of TRDs over the last 200 years.

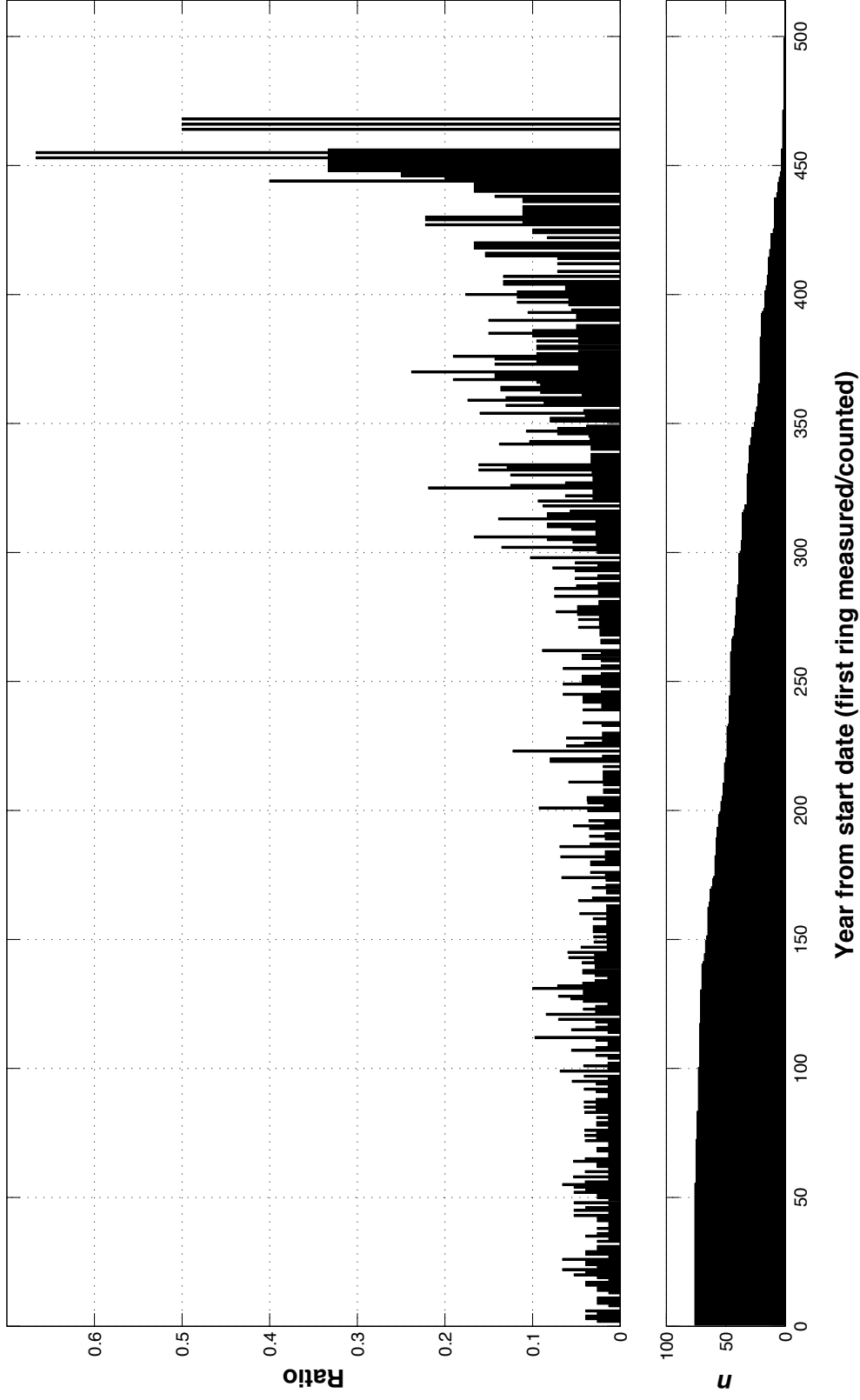


Figure 12. Age distribution of rings in trees at Diamond Peak and Reading Peak (combined) showing evidence of TRDs.

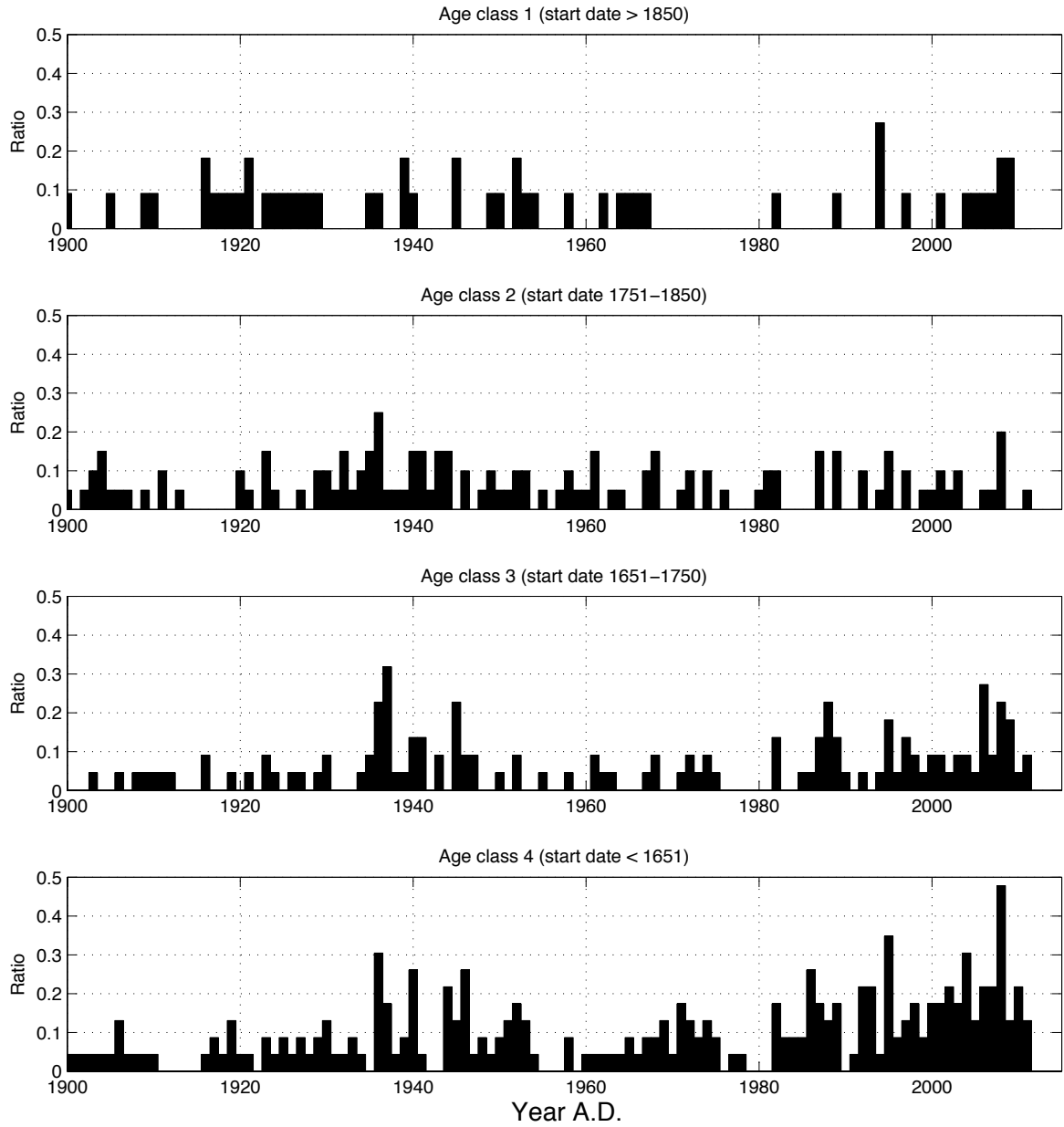


Figure 13. Ratio of trees at Diamond Peak and Reading Peak (combined) showing evidence of TRDs during the 20th and early 21st century by age class. TRDs in age class 4 are more numerous and also show an increase over the last three decades.

Shasta red fir growth – climate relationship

All chronologies (of different standardization choices) were compared to the climate data; however, here we present results based on the comparisons with tree-ring measurements standardized with a 200% cubic spline. Local USHCN station data were used in all cases where the site chronology was located within 50 km from the climate station. Reading Peak and Diamond Peak did not meet this criterion and the climate data from the closest station (Susanville, California) show significant differences from the gridded PRISM product near the tree-ring sites. PRISM data were therefore used in the climate-growth comparison at these two sites.

The Cinnamon Butte record, which is derived from the lowest-elevation and most northerly site, is significantly positively correlated with precipitation in the early summer (May and June), but negatively associated with precipitation in August (**Figure 14A**). It also exhibits a modest positive correlation with minimum temperature in May. When climate variables are combined over longer periods, this association with precipitation dampens out (becomes non-significant), while the positive correlation with early-summer temperatures persists over 3-month and (at a lower significance level, $\alpha = 0.05$) 6-month periods. The Grey Back Meadow record shows few significant correlations with precipitation and minimum temperature (**Figure 14B**). The chronology is significantly ($\alpha = 0.01$) negatively correlated with August precipitation, but over any longer period of time the relationship is non-significant. A significant ($\alpha = 0.05$) negative correlation with minimum temperature over 3-month ending in previous September is also present.

The chronology from Mount Ashland shows significant ($\alpha = 0.05$) positive correlations with January and July precipitation sums, as well as a negative correlation September precipitation (**Figure 14C**). Precipitation sums with a 12-month window show significant positive correlations with previous fall (August ($\alpha = 0.01$), September and October ($\alpha = 0.05$)) as well as current January, February, April and May ($\alpha = 0.05$). No significant correlations were found between minimum temperature and the Mount Ashland record. The Shasta Grey Butte chronology, made up of samples from the highest elevation site, show significant ($\alpha = 0.01$) positive correlations with May minimum temperature (**Figure 14D**). The significant correlation is present when extending the period of comparison to three months (ending in April and May) and six months (ending in May). The Shasta Grey Butte record and 12-month precipitation sums ending in previous August, September, October, November, December, and current January and February are also correlated significantly ($\alpha = 0.01$) positively. No significant correlations were found with local SWE data.

The record from Reading Peak correlates significantly ($\alpha = 0.05$) positively with prior August precipitation (**Figure 14E**). The relationship persists, and amplifies ($\alpha = 0.01$), when the precipitation is extended to 3-month (ending in prior August), 6-month (ending in prior August) and 12-month (ending in prior August, September, October, November, December, and current January and February) periods. Negative significant correlations ($\alpha = 0.05$) with minimum temperature are also present. The Diamond Peak chronology, constructed from samples not far from Reading Peak, shows weaker correlations with precipitation for the shorter periods but a significant

($\alpha = 0.01$) positive relationship exist with 12-month precipitation sums ending in prior August, September, October and November (**Figure 14F**). The previous years late summer precipitation show significant negative correlations ($\alpha = 0.01$) with the record.

The Shasta Grey Butte record shows the highest correlation of any chronology with a climate variable ($r = 0.54$, 6-month minimum temperature ending in September). The divisional climate data (precipitation, temperature, PDSI, and PHDI) were compared to both regional averages of tree growth and individual chronologies but no correlations exceed those reported above. Common significant positive correlations ($\alpha = 0.01$) with the 12-month precipitation sum ending in prior August is exhibited by the four southern-most site chronologies. Similar results were obtained for 12-month precipitation sums ending in prior September and October. Shasta Grey Butte and Cinnamon Butte show significant ($\alpha = 0.01$) positive correlations with May minimum temperature and 3-month minimum temperature average ending in May.

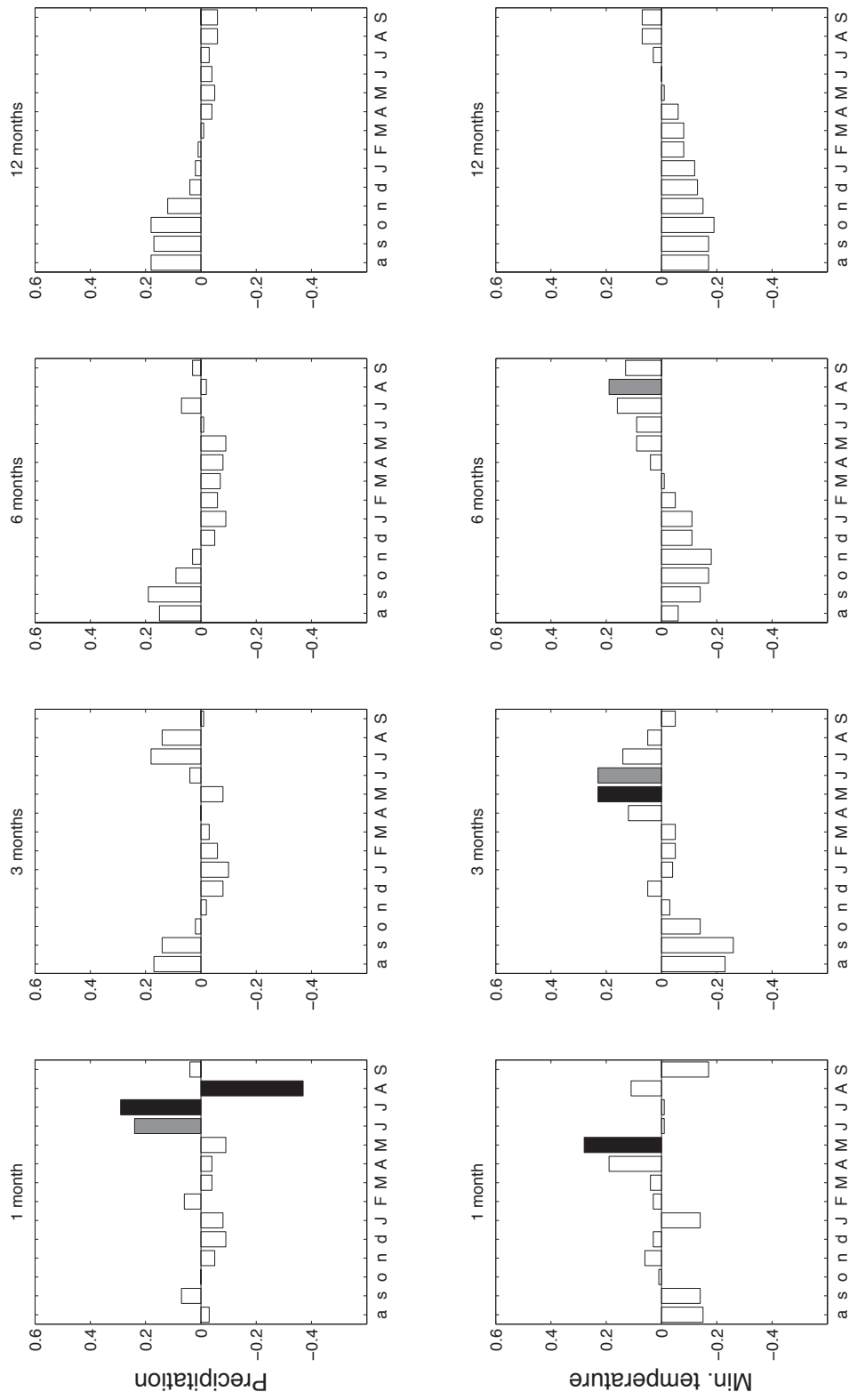


Figure 14A. Correlations between the Cinnamon Butte chronology and total monthly precipitation (upper row) and average minimum temperature (lower row) at Crater Lake, Oregon. Correlations are calculated over the period 1897 to 2011. Correlations significant at the 0.05 and 0.01 level are represented by grey and black shading respectively.

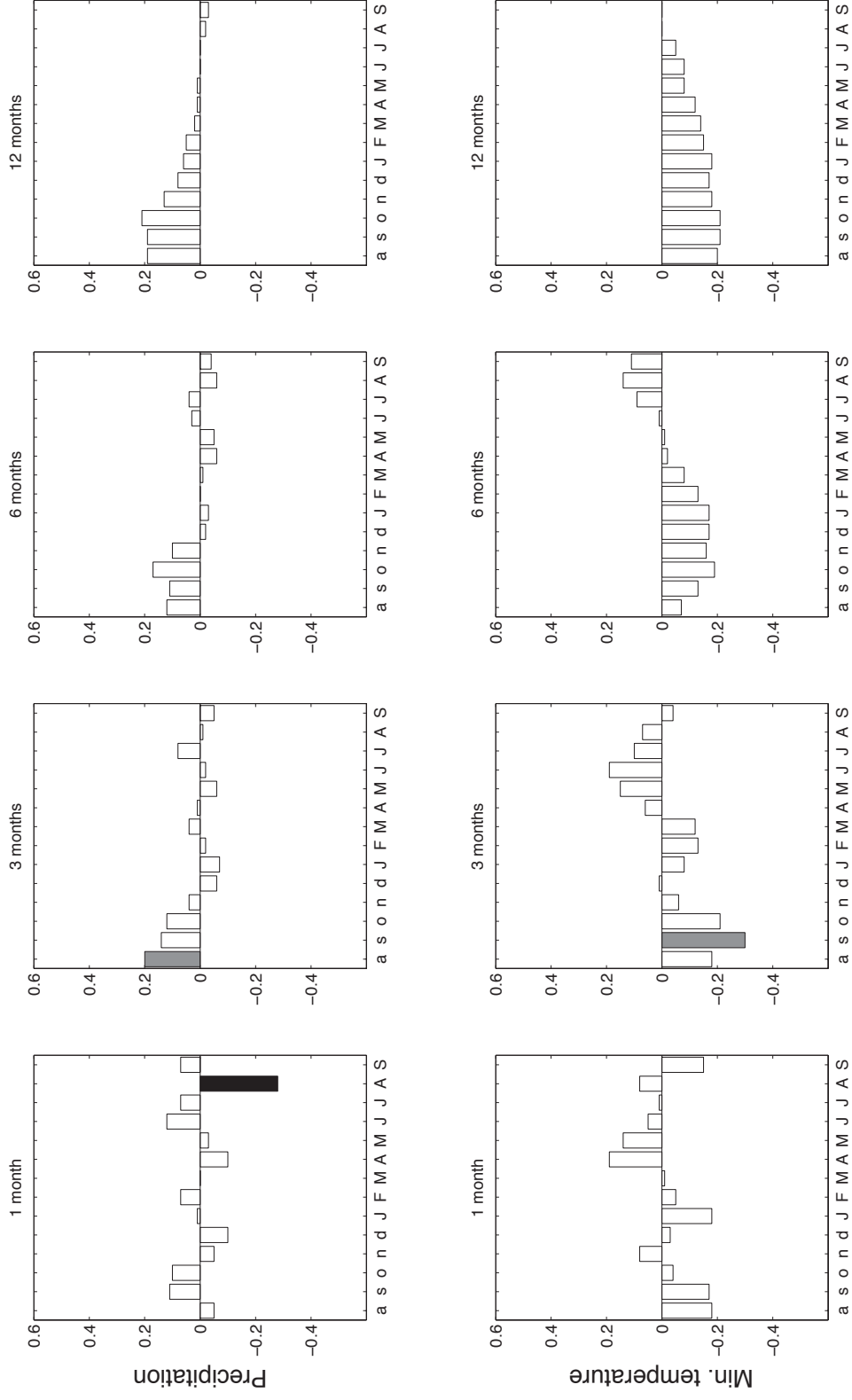


Figure 14B. Correlations between the Grey Back Meadow chronology and total monthly precipitation (upper row) and average minimum temperature (lower row) at Crater Lake, Oregon. Correlations are calculated over the period 1897 to 2011. Correlations significant at the 0.05 and 0.01 level are represented by grey and black shading respectively.

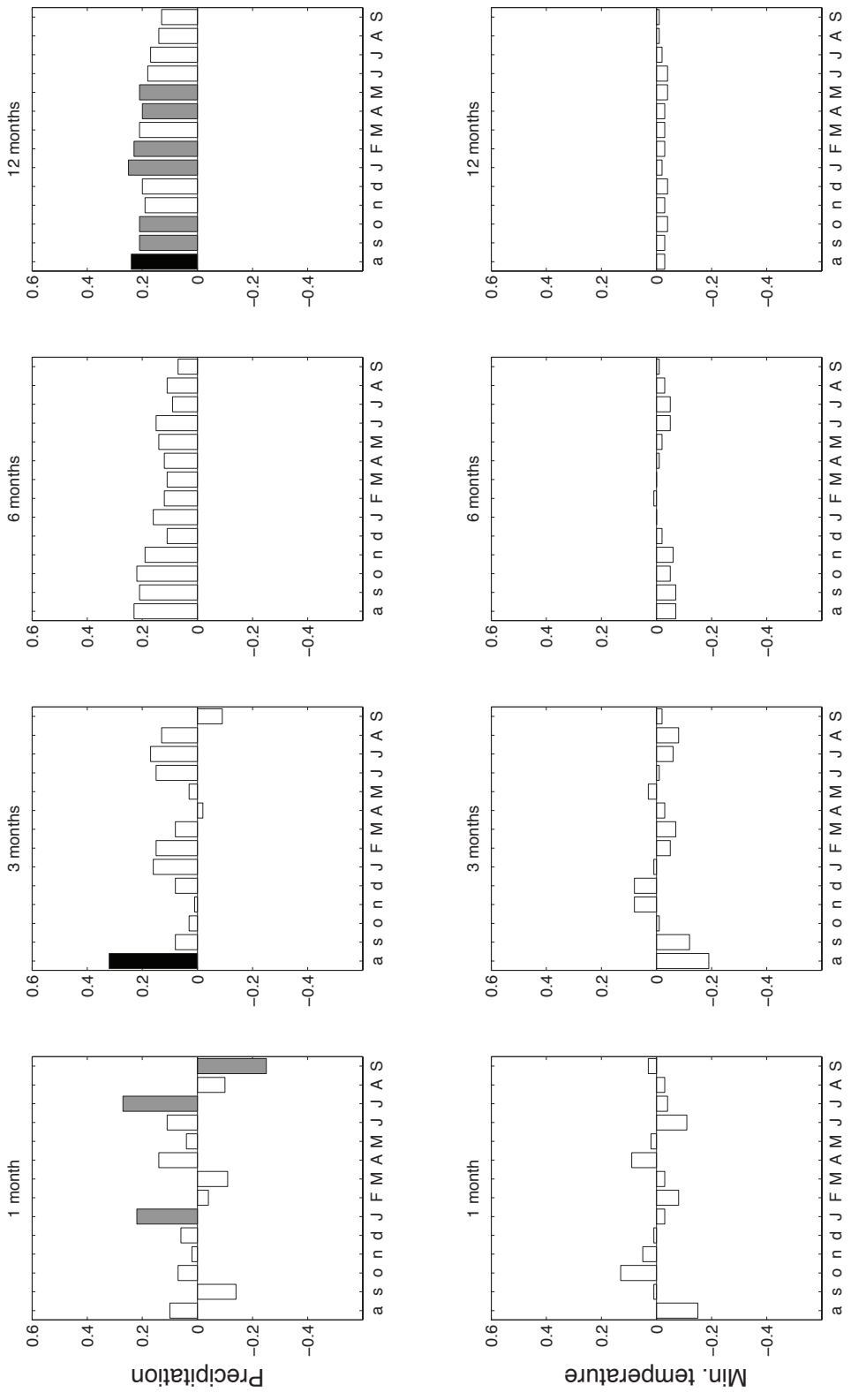


Figure 14C. Correlations between the Mount Ashland chronology and total monthly precipitation (upper row) and average minimum temperature (lower row) at Mount Ashland, Oregon. Correlations are calculated over the period 1897 to 2011. Correlations significant at the 0.05 and 0.01 level are represented by grey and black shading respectively.

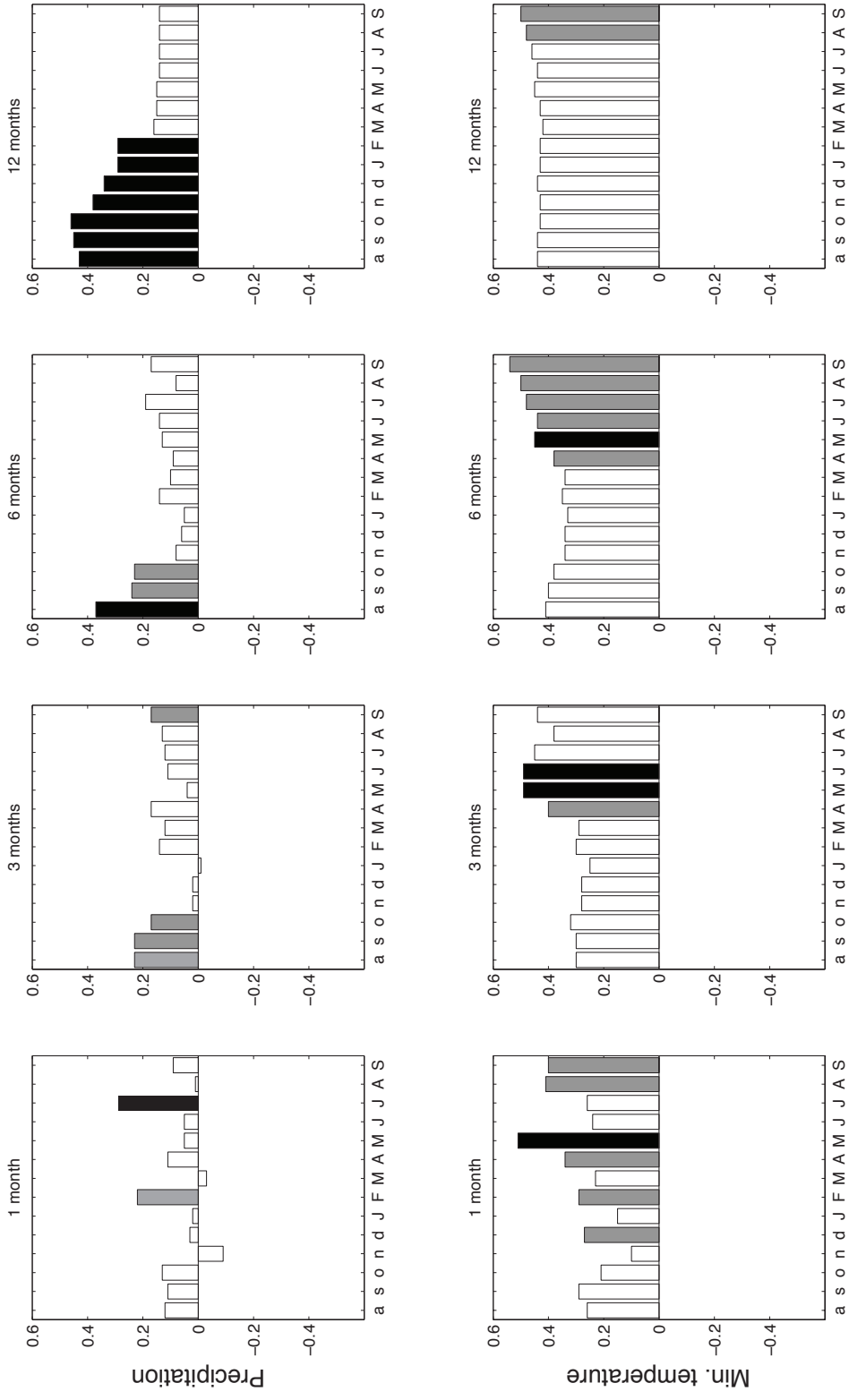


Figure 14D. Correlations between the Shasta Grey Butte chronology and total monthly precipitation (upper row) and average minimum temperature (lower row) at Mount Shasta, California. Correlations are calculated over the period 1897 to 2011. Correlations significant at the 0.05 and 0.01 level are represented by grey and black shading respectively.

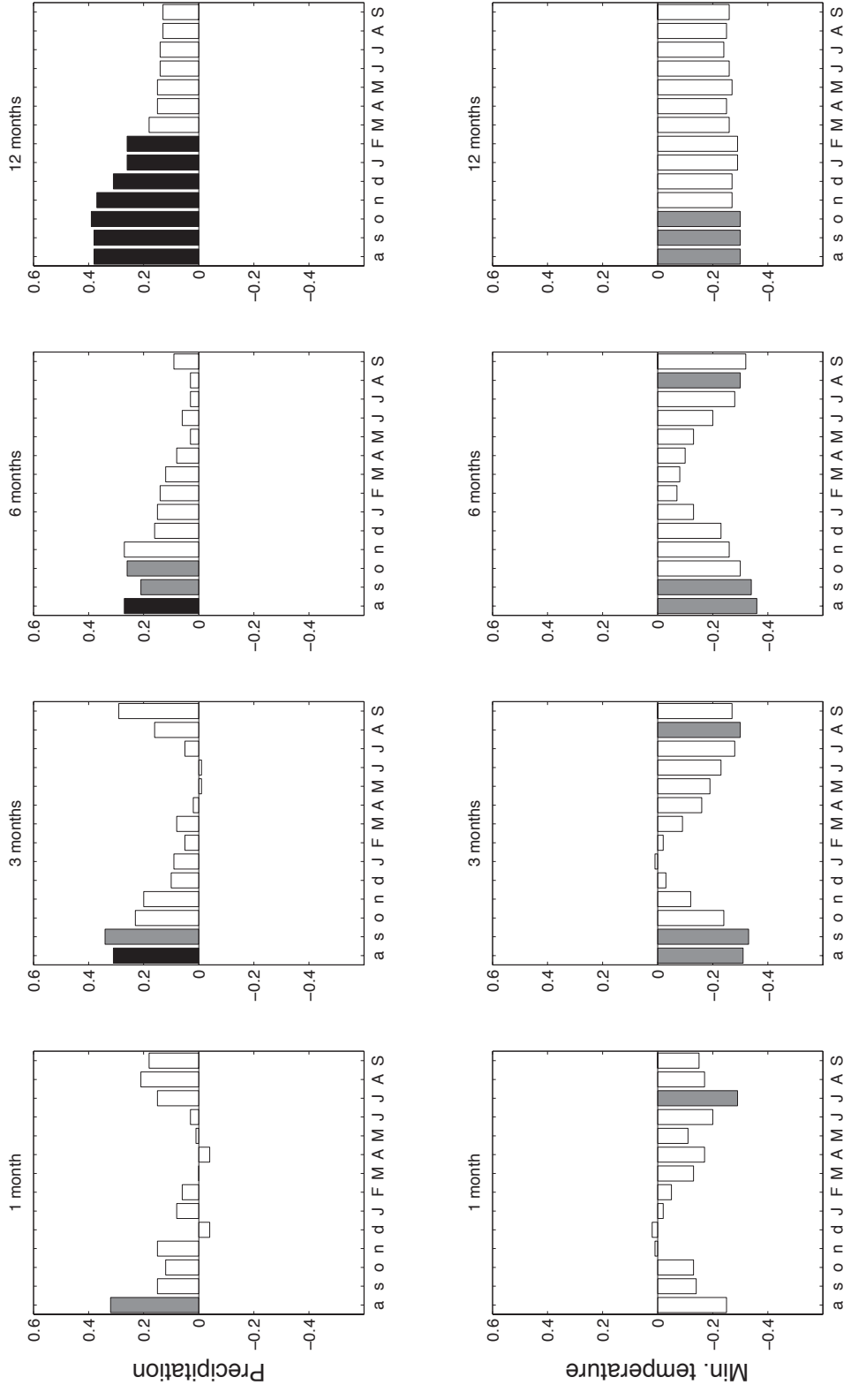


Figure 14E. Correlations between the Reading Peak chronology and total monthly precipitation (upper row) and average minimum temperature (lower row) from PRISM data near Lassen Peak, California. Correlations are calculated over the period 1897 to 2011. Correlations significant at the 0.05 and 0.01 level are represented by grey and black shading respectively.

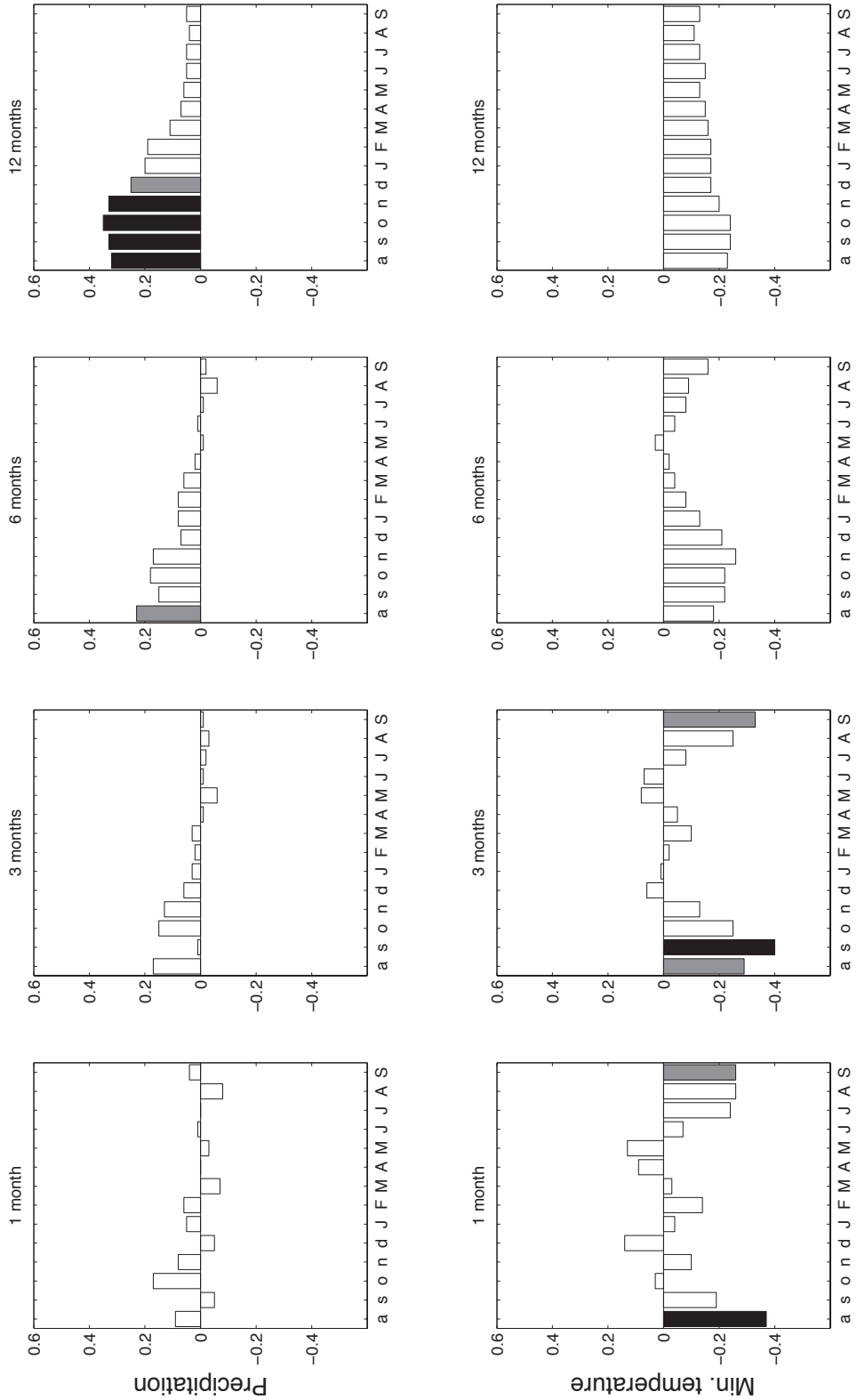


Figure 14F. Correlations between the Diamond Peak chronology and total monthly precipitation (upper row) and average minimum temperature (lower row) from PRISM data near Lassen Peak, California. Correlations are calculated over the period 1897 to 2011. Correlations significant at the 0.05 and 0.01 level are represented by grey and black shading respectively.

DISCUSSION

In this paper, we describe the first multi-site network of tree-ring chronologies developed from Shasta red fir. The replication of records allows us to explore potential associations between the growth of the species and climate in more detail than previous studies. In addition, some inferences can be made about overall stand composition and age. The oldest tree included in our collection (CIB026 from Cinnamon Butte, Oregon) has an inner ring date of A.D. 1340, making it seven years older than the oldest red fir previously reported (Brown 1996). Pith was not present in the CIB026 sample, nor was any curvature of the inner rings that would allow us to estimate the number of rings until pith. It is plausible that the tree exceeds 700 years of age. Oosting and Billings (1943) suggested that it takes up to 500 years for red fir stands to reach their mature dominant state. The authors base this proposition on ring counts from average-sized tree stumps at a site in Washoe County, Nevada. Barbour and Woodward (1985) examined 30 stands of red fir and Shasta red fir at two sites in California and developed formulae relating age to DBH. When the formula for their northern site (closest to the six red fir sites studied in this paper) is applied to our data, the predicted age is consistently greater than the observed ring counts (**Figure 15**). It should be noted that our data lack pith estimates and that the ring counts underestimate the true age of the tree. However, this underestimation cannot alone explain the average of 213 years difference between predicted age and observed ring count. It is possible that our sample strategy of targeting open-grown trees may have removed some stress from competition that trees in denser stands experience. Nonetheless, our results demonstrate that trees 200 years or younger can reach sizes

twice that of considerably older trees. Tree mortality is partly influenced by size, and trees that survive the longest tend to have slower growth rates (Huntington 1913; Melvin 2004). The weak relationship between DBH and observed estimated age (ring count) (**Figure 5**) indicates that size may not be an appropriate surrogate for red fir stand age. Although there are 400 and 500 year old trees in the northern red fir forests, these individuals do not make up the majority of large, dominant trees.

Previous research on other species (Schweingruber 2007; Stoffel 2008) suggests that TRDs are a defense mechanism against one of several possible stresses. If this suggestion also holds true for red fir, records of TRDs could provide a valuable source of information on the frequency of such a stress during past centuries. However, we cannot provide a casual explanation to the presence of the growth anomaly in trees sampled at our five sites. The location of TRDs in the tree-rings indicates that the anomaly formed during the early part of the growing season, most likely no later than July. Our results suggest that TRDs do not occur consistently across the whole circumference of the tree and cross-section samples could potentially bring greater clarity on the formation of these features.

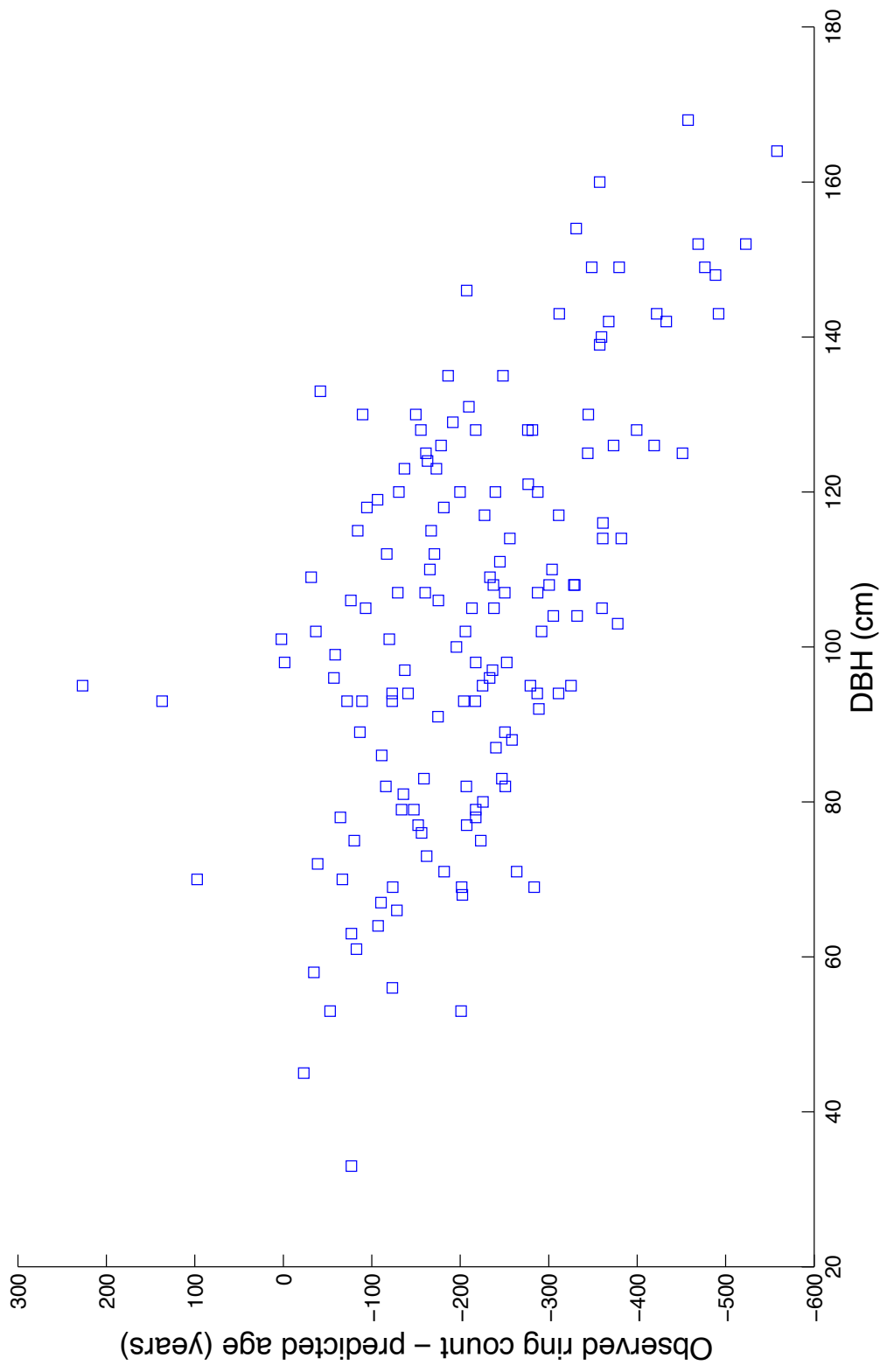


Figure 15. Observed ring count minus predicted age (Barbour and Woodward 1985) derived from DBH. The ring counts are consistently smaller than the predicted age.

Interpreting the climate signal in Shasta red fir

We examined the climate-tree growth relations in six Shasta red fir records from across the species' latitudinal range. Four site chronologies record significant positive correlations with prior water year's precipitation sum. The response is relatively weak ($r = 0.24-0.43$) but consistent across the southern sites, which suggest the relationship between red fir growth and precipitation during the previous year may be meaningful. Trees can allocate energy to next season's growth but dry conditions during summer can restrict photosynthesis and force the tree to divert stored energy to the current year's growth (Fritts 1976). For example, *Abies lasiocarpa* trees in Colorado have recorded positive correlations with precipitation during the prior growing season (Villalba *et al.* 1994). Other statistically significant correlations between individual site chronologies and single climate variables were also found (e.g. Shasta Grey Butte and May minimum temperature, $r = 0.52$) but these are not consistent across all sites. Single site climate reconstructions could be produced but a one-predictor model would produce the same pattern as the chronology, only as an index. If the correlation between minimum temperature over various periods and TRW at Shasta Grey Butte is not spurious, the reason why the relationship is not present (or not as strong) at other sites could be differences in elevation. Shasta Grey Butte has the highest elevation of the six sites sampled and the instrumental data from the Mount Shasta climate station also show considerably lower average minimum temperatures than any other local climate station in the region. Tree-rings from samples growing near treeline in the Cascade Range have previously been shown to exhibit positive correlations with summer temperature (Graumlich and Brubaker 1986). Other studies (e.g. Salzer *et al.*

2009; Kipfmueller and Salzer 2010; Bunn *et al.* 2011) have shown that the sensitivity of radial growth to temperature decreases as elevation drops. A large majority of five-needle pine chronologies that show positive correlations with temperature are treeline sites (Kipfmueller and Salzer 2010). The two southernmost chronologies (from Diamond Peak and Reading Peak) show no positive correlations with any minimum temperature variable. These differences within the region may explain why stronger correlations were not found between regionally averaged tree-rings and climate variables. It may be that red fir growth at the species' highest elevational and latitudinal range is limited by temperature to a greater extent. Sampling several red fir stands across an elevational transect on a mountain side could yield further insight (Bunn *et al.* 2011); however finding a suitable site may prove difficult. Our observations during fieldwork suggests that open-grown trees are not present all elevations.

The relationship with past precipitation at our southern sites indicates that trees could be responding to several independent climate variables over a long period of time, and that TRW at these sites may represent both past and present conditions. If the end of the growing season is not dry, stored energy may mediate some of the possible stress during the following growing season. We examined the lowest ten years of growth at Shasta Grey Butte during the period of instrumental climate data (1896-2011). Shasta Grey Butte was chosen because the chronology has the highest correlation with a current year climate variable. In nine of the years, the previous water year's precipitation was below average. In eight of the years, the current May minimum temperature was below average. In seven of the years, both past

precipitation and current temperature were below average, including four of the five years of lowest growth. Modeling of tree-growth (as described by Vaganov *et al.* 2006 and Evans *et al.* 2006) could reveal further insight to the potential multivariate impact of climate on Shasta red fir.

Although no single climate variable appears to control tree growth at all six sites, the common pattern in TRW exhibited by the site chronologies suggests that there is a regional forcing of growth. The complicated relationship between winter precipitation, early summer temperature, and snowpack may affect any potential climate signal in the trees (Graumlich and Brubaker 1986). Deep or lingering snowpack could delay the onset of growing season and thus limit radial growth. Peterson and Peterson (2001) found that mountain hemlock growth at Crater Lake, Oregon (within 2 km from Grey Back Meadow), was negatively correlated with spring snowpack. However, the CPC receive low amounts of precipitation during the summer months and moisture availability during late summer could also limit growth. Conifers in northern California and southern Oregon have previously been used to reconstruct past drought conditions (e.g. Graumlich 1987). Since winter precipitation is the major source of soil water recharge in the region, snow pack may therefore have both a negative and positive effect on red fir growth depending on the phase of the growing season. Such dual response would be difficult to disentangle in our data. Seasonal climate signals in tree-rings have been recorded successfully in trees with distinct earlywood-latewood boundaries (Griffin *et al.* 2011) but the samples we have collected lack such features.

CONCLUSION

We are able to show that Shasta red fir shares some common variability in inter-annual radial growth across the latitudinal range of the species, making it possible to cross-date trees over short distances (<50 km). This regional forcing is likely climatic in nature, however, no single climate variable tested can explain a significant amount of the variance in all six records. Our findings do not support the prior suggestion that red fir growth is primarily controlled by minimum temperature. Rather, we argue that any climate signal in the trees is multivariate and not limited to a single month, and that the relationship between climate and red fir growth may involve both elevational and latitudinal factors. Correlations between our six chronologies, as well as the relationship between individual chronologies and local climate data, indicate that there may be a distinct difference between northern and southern sites. In addition, growth may not only be influenced by the current year's climate but also affected by the tree's ability to store resources from the prior year.

The ring counts of large trees in our collection are considerably lower than what can be expected based on previous studies. Shasta red fir forests in our study region contain trees of a wide range of ages, regardless of the trees' sizes. It is likely that parts of the red fir stands in northern California and southern Oregon are considerably younger than previously estimated. To further assess stand dynamics and age, we recommend the inclusion of dendrochronological techniques in future studies.

Future research

There are still many unanswered questions regarding the relationship between red fir growth and climate variability. A transect of red fir stands at different elevations along a mountain side would allow testing if temperature is a driver of ring-width variability only near tree-line. However, finding single stands with relatively open-grown trees proved difficult during our fieldwork and such an elevational transect may not be possible to construct. Our experiences suggest that Mount Shasta, California, and Mount Ashland, Oregon, have the highest probability of yielding suitable stands.

Similar to the latitudinal range of sites analyzed above, a longitudinal gradient could provide insight into the influence of moisture on red fir growth. Previous observations indicate that red firs in western Nevada grow at a seemingly lower rate than those studied here. Trees west of the rain-shadow are more likely to be moisture stressed and therefore may not store energy for the upcoming year. Samples from both sides of the Southern Cascades could therefore prove beneficial for understanding whether the lagged correlation recorded between precipitation of the previous water year and our ring widths is causal or spurious.

Further work on red fir should also attempt to find subfossil trees. Older material would allow for an extension of the current chronologies further back in time, but also contribute with more information on TRDs. We were unable to find any causal factor(s) behind the TRDs present in many of the samples but it is not possible to rule out age as the driver of the trend at the two southern sites unless trees that died

prior to the last 100 years are studied. Unfortunately, the environments that red firs grow in are not conducive to preserving wood well.

REFERENCES

- Ault, T.R. and S. St. George 2010 “The magnitude of decadal and multidecadal variability in North American precipitation” *Journal of Climate*, **23**, 842-850.
- Barbour, M.G. and R.A. Woodward “The Shasta red fir forest of California” *Canadian Journal of Forest Research*, **15**, 570-576.
- Bradley, R.S. 1985 *Quaternary Paleoclimatology – Methods of Paleoclimatic Reconstruction*, Allen & Unwin Inc., Winchester, MA.
- Bradley, R.S. 2008 “Holocene perspectives on future climate change” in Battarbee, R.W. and Binney, H.A. (Eds.) *Natural Climate Variability and Global Warming: A Holocene Perspective*, Blackwell Publishing Ltd, Oxford.
- Briffa, K.R., P.D. Jones and F.H. Schweingruber 1992 “Tree-ring density reconstructions of summer temperature patterns across western North America since 1600” *Journal of Climate*, **5**, 735-754.
- Brown, P.M. 1996 “OLDLIST: A database of maximum tree ages” in Dean, J.S., Meko, D.M. and Swetnam T.W. (Eds.) *Tree rings, environment, and humanity*, Radiocarbon, University of Arizona, Tucson, AZ.
- Bunn, A.G., M.K. Hughes and M.W. Salzer 2011 “Topographically modified tree-ring chronologies as a potential means to improve paleoclimate inference” *Climatic Change*, **105**, 627-634.
- Cayan, D.R., K.T. Redmond and L.G. Riddle 1999 “ENSO and hydrological extremes in the western United States” *Journal of Climate*, **12**, 2881-2893.
- CDEC *Snow Course Data*, California Data Exchange Center – Department of Water Resources, Web, (accessed: 14 Mar. 2013).
- Conover, W.J. 1980 *Practical Nonparametric Statistics*, John Wiley & Sons, Hoboken NJ.
- Cook, E.R. and R.L. Holmes 1986 *Users manual for program ARSTAN*, Laboratory of Tree-Ring Research, University of Arizona, Tucson AZ.
- Crawford, C.J. 2012 “Do high-elevation northern red oak tree-rings share a common climate-driven growth signal?” *Arctic, Antarctic and Alpine Research*, **44**, 26-35.

- Daly, C., M. Halbleib, J.I. Smith, W.P. Gibson, M.K. Doggett, G.H. Taylor, J. Curtis and P.P. Pasteris 2008 “Physiographically sensitive mapping of climatological temperature and precipitation across the conterminous United States” *International Journal of Climatology*, **28**, 2031-2064.
- Dettinger, M.D. 2011 “Climate change, atmospheric rivers, and floods in California – A multimodel analysis of storm frequency and magnitude changes” *Journal of the American Water Resources Association*, **47**, 514-523.
- Evans, M.N., B.K. Reichert, A. Kaplan, K.J. Anchukaitis, E.A. Vaganov, M.K. Hughes, and M.A. Cane 2006 “A forward modeling approach to paleoclimatic interpretation of tree-ring data” *Journal of Geophysical Research: Biogeosciences*, **111**, doi: 10.1029/2006JG000166
- Florsheim, J.L. and M.D. Dettinger 2007 “Climate and floods still govern California levee breaks” *Geophysical Research Letters*, **34**, doi: 10.1029/2007GL031702
- Fritts, H.C. 1976 *Tree Rings and Climate*. Academic Press, London, UK.
- Gedalof, Z., D.L. Peterson and N.J. Mantua 2004 “Columbia River flow and drought since 1750” *Journal of the American Water Resources Association*, **40**, 1579-1592.
- Gordon, D.T. 1979 “Successful natural regeneration cuttings in California true firs” *Forest Service Research Paper PSW*, **140**, 1-20.
- Graumlich, L.J. 1987 “Precipitation variation in the Pacific Northwest (1675-1975) as reconstructed from tree rings” *Annals of the Association of American Geographers*, **77**, 19-29.
- Graumlich, L.J. 1993 “A 1000-year record of temperature and precipitation in the Sierra Nevada” *Quaternary Research*, **39**, 249-255.
- Graumlich, L.J. and L.B. Brubaker 1986 “Reconstruction of Annual Temperature (1590-1979) for Longmire, Washington, Derived from Tree Rings” *Quaternary Research*, **25**, 223-234.
- Griffin, D.R., D.M. Meko, R. Touchan, S.W. Leavitt and C.A. Woodhouse 2011 “Latewood chronology development for summer-moisture reconstruction in the US southwest” *Tree-Ring Research*, **67**, 87-101.
- Grissino-Mayer, H.D. and H.C. Fritts 1997 “The International Tree-Ring Data Bank: An enhanced global database serving the global scientific community” *Holocene*, **7**, 228-235.

- Higgins, R.W., V.B.S. Silva, W. Shi and J. Larson 2007 “Relationships between climate variability and fluctuations in daily precipitation over the United States” *Journal of Climate*, **20**, 3561-3579.
- Holmes, R.L. 1986 “Users manual for program COFECHA” in Holmes, R.L., Adams, R.K., Fritts, H.C. (Eds.) *Tree-ring Chronologies of Western North America: California, Eastern Oregon, and Northern Great Basin*, Laboratory of Tree-Ring Research, University of Arizona, Tucson AZ, 41-49.
- Huntington, E. 1913 *The secret of big trees*. Department of Interior, Washington DC.
- Kipfmüller, K.F. and M.W. Salzer 2010 “Linear trend and climate response of five-needle pines in the western United States related to treeline proximity” *Canadian Journal of Forest Resources*, **40**, 134-142.
- McCabe, G.J., J.L. Betancourt and H.G. Hidalgo 2007 “Associations of decadal to multidecadal sea-surface temperature variability with upper Colorado River flow” *Journal of the American Water Resources Association*, **43**, 183-192.
- Meko, D.M., R. Touchan and K.J. Anchukaitis 2011 “Seascorr: A MATLAB program for identifying the seasonal climate signal in an annual tree-ring time series” *Computers & Geosciences*, **37**, 1234-1241.
- Melvin, T.M. 2004 *Historical growth rates and changing climatic sensitivity of boreal conifers*, PhD thesis, University of East Anglia, Norwich, UK.
- Menne, M.J., C.N. Williams Jr. and R.S. Vose 2009 “The U.S. historical climatology network monthly temperature data, Version 2” *Bulletin of American Meteorological Society*, **90**, 993-1007.
- Oosting, H.J. and W.D. Billings 1943 “The red fir forest of the Sierra Nevada: *Abietum Magnificae*” *Ecological Monographs*, **13**, 259-274.
- Peterson, D.W. and D.L. Peterson 2001 “Mountain hemlock growth responds to climatic variability at annual and decadal time scales” *Ecology*, **82**, 3330-3345.
- Peterson, D.W., D.L. Peterson and G.J. Ettl 2002 “Growth responses of subalpine fir to climatic variability in the Pacific Northwest” *Canadian Journal of Forest Research*, **32**, 1503-1517.
- Riegel, G.M., R.F. Miller, C.N. Skinner and S.E. Smith 2006 “Northeastern plateaus bioregion” in Sugihara N.G., van Wagendonk, J., Shaffer, K.E., Fites-Kaufman, J., and Thode, A.E. (Eds.) *Fire in California's Ecosystems*. University of California Press, Berkeley CA, 225-263.

- Rocheford, R.M., R.L. Little, A. Woodward and D.L. Peterson 1994 “Changes in sub-alpine tree distribution in western North America: a review of climatic and other causal factors” *Holocene*, **4**, 89-100.
- Royce, E.B. and M.G. Barbour 2001 “Mediterranean climate effects. II. Conifer growth phenology across a Sierra Nevada ecotone” *American Journal of Botany*, **88**, 919-932.
- St. George, S. and T.R. Ault 2011 “Is energetic decadal variability a stable feature of the central Pacific Coast’s winter climate?” *Journal of Geophysical Research*, **116**, doi: 10.1029/2010JD015325
- St. George, S. and T.R. Ault 2014 “The imprint of climate within Northern Hemisphere trees” *Quaternary Science Reviews*, **89**, 1-4.
- Salzer, M.W., M.K. Hughes, A.G. Bunn and K.F. Kipfmüller 2009 “Recent unprecedented tree-ring growth in bristlecone pine at the highest elevations and possible causes” *Proceedings of the National Academy of Sciences of the United States of America*, **106**, 20348-20353.
- Sawyer, J.O. and D.A. Thornburg 1988 “Montane and subalpine vegetation of the Klamath Mountains” in Barbour, M.G. and Major, J. (Eds.) *Terrestrial vegetation of California*, Special Publication No. 9, California Native Plant Society, Berkeley CA, 699-732.
- Schweingruber, F.H. 1988 “A new dendroclimatic network for western North America” *Dendrochronologia*, **6**, 171-180.
- Schweingruber, F.H. 2007 *Wood Structure and Environment*, Springer-Verlag, Berlin.
- Skinner, C.N. and A.H. Taylor 2006 “Southern Cascades Bioregion” in Sugihara, N.G., van Wageningen J.W., Shaffer, K.E., Fites-Kaufman, J. and Thode A.E. (Eds.) *Fire in California’s Ecosystems*. University of California Press, Berkeley.
- Stahle, D.W., D.R. Griffin, M.K. Cleaveland, J.R. Edmondson, F.K. Fye, D.J. Burnette, J.T. Abatzoglou, K.T. Redmond, D.M. Meko, M.D. Dettinger, D.R. Cayán and M.D. Therrell 2011 “A tree-ring reconstruction of the salinity gradient in the northern estuary of San Francisco Bay” *San Francisco Estuary & Watershed Science*, **9**, 1-24.
- Stoffel, M. 2008 “Dating past geomorphic processes with tangential rows of traumatic resin ducts” *Dendrochronologia*, **26**, 53-60.

- Stokes, M.A. and T.L. Smiley 1968 *An introduction to tree-ring dating*, The University of Chicago Press, Chicago IL.
- Touchan, R., D.M. Meko, J.A. Ballesteros-Cánovas, R. Sánchez-Salguero, J.J. Camarero, D. Kerchouche, E. Muntan, M. Khabcheche, J.A. Blanco, C.R. Morata, V. Garófano-Gómez, L.A. Martín, R. Alfaro-Sánchez, K. Garah, A. Hevia, J. Madrigal-González, A. Sánchez-Miranda, T.A. Shestakova and M. Tabakova 2013 “Dendrochronology course in Valsain Forest, Segovia, Spain” *Tree-Ring Research*, **69**, 93-100.
- Vaganov, E.A., M.K. Hughes and A.V. Shashkin 2006 *Growth Dynamics of Tree Rings: Images of Past and Future Environment*, Springer, New York.
- Villalba, R., T.T. Veblen and J. Ogden 1994 “Climatic influences on the growth of subalpine trees in the Colorado Front Range” *Ecology*, **75**, 1450-1462.
- Westhusing, J.K. 1973 “Reconnaissance surveys of near-event seismic activity in the volcanoes of the Cascade Range, Oregon” *Bulletin of Volcanology*, **37**, 258-286.
- Wigley, T.M.L., K.R. Briffa and P.D. Jones 1984 “On the average value of correlated time series, with applications in dendroclimatology and hydrometeorology” *Journal of Climate and Applied Meteorology*, **23**, 201-213.
- Wise, E.K. 2010 “Spatiotemporal variability of the precipitation dipole transition zone in the western United States” *Geophysical Research Letters*, **37**, doi: 10.1029/2009GL042193
- Yamaguchi, D.K. 1986 “Interpretation of cross correlation between tree-ring series” *Tree-Ring Bulletin*, **46**, 47-54.
- Zhang, J. and W.W. Oliver 2006 “Stand structure and growth of *Abies magnifica* responded to five thinning levels in northeastern California, USA” *Forest Ecology and Management*, **223**, 275-283.